Manipulation of Organoactinide Coordinative Unsaturation. Synthesis, Structures, and Reactivity of Thorium Hydrocarbyls and Hydrides with Chelating Bis(tetramethylcyclopentadienyl) Ancillary Ligands

Carol M. Fendrick,[1a] Larry D. Schertz,[1a] Victor W. Day,*[,1b] and Tobin J. Marks*[,1a]

Department of Chemistry, Northwestern University, Evanston, Illinois 60208, Crystalytics Company, Lincoln, Nebraska 68501, and Department of Chemistry, University of Nebraska, Lincoln, Nebraska 68588

Received February 11, 1988

This contribution describes thorium hydrocarbyl and hydride chemistry based upon the chelating $(CH_3)_2Si[(CH_3)_4C_5]_2^{2-}$ ligand ($Me_2SiCp''_2^{2-}$). Precursor $Me_2Si(Cp''H)_2$ can be prepared by reaction of $SiCl_4$ with 2 equiv of $Li(CH_3)_4C_5$, followed by methylation (CH_3Li) and methanolic workup. Subsequent reaction with n-C_4H_9Li in 1,2-dimethoxyethane yields $Me_2Si(Cp''Li)_2 \cdot 2DME$. The dilithium salt undergoes reaction with $ThCl_4$ to yield $Me_2SiCp''_2ThCl_2 \cdot 2LiCl \cdot 2DME$, which, in turn, can be alkylated with lithium reagents to produce crystalline, thermally stable $Me_2SiCp''_2ThR_2$ complexes where R = $CH_2Si(CH_3)_3$, $CH_2C(CH_3)_3$, C_6H_5, n-C_4H_9, and $CH_2C_6H_5$. The $Me_2SiCp''_2Th[CH_2Si(CH_3)_3]_2$ complex crystallizes in the monoclinic space group $P2_1/m$—C_{2h}^2 with two molecules in a unit cell of dimensions (20 ± 1 °C) a = 11.960 (5) Å, b = 11.270 (5) Å, c = 12.395 (6) Å, and β = 99.32 (4)°. Least-squares refinement led to a value for the conventional R index (on F) of 0.076 for 2586 independent reflections having $I > 3\sigma(I)$. The molecular structure consists of monomeric $Me_2SiCp''_2Th[CH_2Si(CH_3)_3]_2$ units with η^5-Cp'' coordination and ∠ (ring centroid)–Th–(ring centroid) = 118.4°. There is considerable dispersion in the Th–C(ring) distances. The $Th[CH_2Si(CH_3)_3]_2$ ligation is highly distorted, with Th–C–Si angles of 123.7 (14)° and 149.5 (12)°, accompanied by corresponding Th–C distances of 2.54 (2) and 2.48 (2) Å, respectively. The thorium coordination sphere is more "open" than that in $Cp'_2Th[CH_2Si(CH_3)_3]_2$. Hydrogenolysis of the dialkyl yields the dimeric hydride $Me_2SiCp''_2Th(\mu\text{-}H)_4ThCp''_2SiMe_2$, which crystallizes in the monoclinic space group $P2_1/n$ with four molecules in a unit cell of dimensions (20 ± 1 °C) a = 10.965 (2) Å, b = 19.843 (5) Å, c = 18.759 (3) Å, and β = 90.39 (2)°. Least-squares refinement led to a value for the conventional R index (on F) of 0.075 for 3298 independent reflections having $I > 3\sigma(I)$. The dimer exhibits approximate C_2 symmetry with (ring centroid)–Th–(ring centroid) angles of 118.1° and 117.7°. The Th–Th distance is 3.632 (2) Å which suggests, in combination with infrared spectral data, a $Th(\mu\text{-}H)_4Th$ structure. The above hydride catalyzes the hydrogenation of 1-hexene at a rate ca. 10^3 faster than $(Cp'_2ThH_2)_2$. For *trans*-2-hexene, hydrogenation catalyzed by the ring-bridged hydride is ca. 30 times more rapid than by $(Cp_2'ThH_2)_2$.

The efficacy of bis(pentamethylcyclopentadienyl) actinide ligation (Cp'_2An, $Cp' = \eta^5$-$(CH_3)_5C_5$, An = actinide) in affording complexes with advantageous solubility, crystallizability, thermal stability, and resistance to ligand redistribution is well-established.[2] However, abundant structural data indicate that these advances are accompanied by a congestion of the metal coordination sphere that may depress reactivity relative to known or hypothetical bis(cyclopentadienyl) analogues.[2] In an effort to "open" the actinide coordination sphere while preserving the frontier orbitals[3] and other advantages of Cp'_2An ancillary ligation, we have synthesized and explored the actinide coordination chemistry of the first chelating bis(permethylcyclopentadienyl) ligand (A, $Me_2SiCp''_2$).[4-6] In

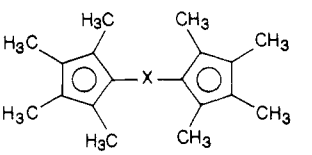

A, X = $Si(CH_3)_2$

this contribution, we present an account of thorium hydrocarbyl and hydride chemistry based upon this ligand. The discussion includes both ligand synthetic as well as organometallic synthetic and homogeneous catalytic details. It is seen that $Me_2SiCp''_2Th$ ligation can effect substantial changes in molecular structure and catalytic reactivity over Cp'_2Th analogues. We discuss in detail the crystal structures of a mononuclear thorium bis(hydrocarbyl) and a dimeric thorium tetrahydride. The latter result features a *very short* Th–Th distance.

Experimental Section

Physical and Analytical Methods. Proton and carbon NMR spectra were recorded on either a JEOL FX-270 (FT, 270 MHz, ^{13}C 67.80 MHz), a JEOL FX-90Q (FT, 90 MHz), a Varian EM-390 (CW, 90 MHz), or a Perkin-Elmer R20-B (CW, 60 MHz) spectrometer. Chemical shifts are reported relative to internal TMS.

(1) (a) Northwestern University. (b) Crystalytics Co. and the University of Nebraska.

(2) (a) Marks, T. J.; Streitwieser, A., Jr. In *The Chemistry of the Actinide Elements*, 2nd ed.; Katz, J. J.; Seaborg, G. T.; Morss, L. R., Eds.; Chapman and Hall: London, 1986; Chapter 22. (b) Marks, T. J. *Ibid.*, Chapter 23. (c) Marks, T. J.; Fragalâ, I., Eds. *Fundamental and Technological Aspects of Organo-f-Element Chemistry*; D. Reidel: Dordrecht, Holland, 1985. (d) Marks, T. J.; Ernst, R. D. In *Comprehensive Organometallic Chemistry*; Wilkinson, G. W.; Stone, F. G. A.; Abel, E. W., Eds.; Pergammon: Oxford, 1982; Chapter 21.

(3) (a) Tatsumi, K.; Nakamura, A. *J. Am. Chem. Soc.* **1987**, *109*, 3195–3206. (b) Tatsumi, K.; Nakamura, A.; Hofmann, P.; Hoffmann, R.; Moloy, K. G.; Marks, T. J. *J. Am. Chem. Soc.* **1986**, *108*, 4467–4476. (c) Bursten, B. E.; Fang, A. *Inorg. Chim. Acta* **1985**, *110*, 153–160 and references therein.

(4) (a) Fendrick, C. M.; Mintz, E. A.; Schertz, L. D.; Marks, T. J.; Day, V. W. *Organometallics* **1984**, *3*, 819–821 (preliminary communication). (b) Presented in part at the 11th International Conference on Organometallic Chemistry, Pine Mountain, GA, Oct 1983, Abstract 84.

(5) For related ligand synthetic studies, see: (a) Jutzi, P.; Dickbreder, R. *Chem. Ber.* **1986**, *119*, 1750–1754. (b) Scholz, H. J.; Werner, H. *J. Organomet. Chem.* **1986**, *303*, C8–C12.

(6) For complementary organolanthanide work, see: Jeske, G.; Schock, L. E.; Swepston, P. N.; Schumann, H.; Marks, T. J. *J. Am. Chem. Soc.* **1985**, *107*, 8103–8110.

0276-7333/88/2307-1828$01.50/0

The solid-state ^{13}C spectrum was recorded on a JEOL FX-60QS (CPMAS, 15 MHz) instrument. Infrared spectra were recorded on Nujol or Fluorolube mulls sandwiched between KBr plates in an O-ring sealed, air-tight holder using a Perkin-Elmer 599B or 283 spectrophotometer. Infrared spectra were calibrated with polystyrene film. Gas chromatography was carried out with a Varian 3700 gas chromatograph using FID and either a 5% SE30 on Chromosorb W or 5% FFAP on Chromosorb G column.

Elemental analyses were performed by Dornis und Kolbe Mikroanalytiches Laboratorium, Mülheim, West Germany.

Materials and Methods. Air-sensitive compounds were handled with rigorous exclusion of oxygen and moisture in Schlenk-type glassware on a dual manifold Schlenk line, in Schlenk-type glassware interfaced to a high vacuum (10^{-5} Torr) system, or under a dinitrogen atmosphere in a Vacuum Atmospheres glovebox with an efficient recirculator. Argon (Matheson, prepurified), dinitrogen (Liquid Air Corp., high purity), hydrogen (Linde), and deuterium gas (Matheson, 99.5%) were purified by passage through sequential columns of MnO and Davidson 4-Å molecular sieves.[7] Reactions with gases were performed in an enclosed volume on the vacuum line. Gas uptake was monitored on a mercury manometer.

Benzene, Et_2O, toluene, heptane, pentane, THF (tetrahydrofuran), and DME (dimethoxyethane) for synthesis were distilled from Na/K/benzophenone under dinitrogen and were condensed and stored in vacuo on the vacuum line in bulbs containing a small amount of $[Ti(Cp)_2Cl]_2ZnCl_2$[8] or Cp'_2UCl_2 as an O_2/H_2O indicator. Toluene solvent for the catalytic hydrogenation of 1-hexane and *trans*-2-hexene was distilled from Na/K alloy immediately before use. Methanol was distilled from magnesium under a nitrogen atmosphere. Chloroform-*d* was dried over P_2O_5 and vacuum transferred to activated Davidson 4-Å molecular sieves. Other deuteriated solvents were dried over Na/K alloy and vacuum transferred before use.

Silicon tetrachloride (Aldrich) was purified by distillation under dinitrogen and freeze–thaw–degassed. The 1-hexene (99%, Aldrich) and *trans*-2-hexene (99+%, Aldrich) were dried by storing over Na/K alloy and were freeze–thaw–degassed. Solutions of isopropylmagnesium chloride in Et_2O (Alfa), *n*-butyllithium in hexane (Aldrich), methyllithium as a lithium bromide complex in Et_2O (Aldrich), and phenyllithium in cyclohexane/Et_2O (Aldrich) were used without further purification.

The lithium reagents $LiCH_2Si(CH_3)_3$[9] and $LiCH_2C(CH_3)_3$[10] were prepared by metalation of the corresponding halides in refluxing pentane. The lithium reagent $LiCH_2C_6H_5$ was prepared from *sec*-butyllithium and toluene.[11] The hydride $[Cp'_2ThH_2]_2$ was prepared by the literature procedure.[12]

2,3,5,6-Tetrahydro-2,3,5,6-tetramethyl-γ-pyrone. This is a modification of the procedure of Burger, Delay, and Mazenod.[13] A 12-L three-necked round-bottom flask fitted with a mechanical stirrer and gas inlet was flushed with dinitrogen. Under a dinitrogen flush, 2360 mL of methanol and 380 g (6.77 mol) of KOH were added to the flask. The solution was then cooled to 0 °C, and 2000 mL (18.9 mol) of 3-pentanone was added under a dinitrogen flush. The solution was maintained at 0 °C, and 4245 mL (75.5 mol) of acetaldehyde was added dropwise with stirring over 36 h. During the addition of acetaldehyde, the solution in the flask changed to a deep red and then to a dark brownish red color. After acetaldehyde addition was complete, the reaction solution was stirred an additional 12 h at 0 °C.

Cold, concentrated HCl, 600 mL, was next added dropwise to the reaction solution at 0 °C. The aqueous and organic layers were then separated, and the organic layer was washed three times with 1 L of 2 N HCl. The aqueous phase was then back-extracted with 2 × 1 L of ether. After the ether was removed by rotary evaporation, the organic layers were combined and washed once with 1 L of 2 N NaCl solution. The methanol was next removed by rotary evaporation, leaving a viscous red oil. Fractional distillation at 70–83 °C (15 Torr) yielded 1780 g (60%) of a clear yellow liquid, which is predominantly 2,3,5,6-tetrahydro-2,3,5,6-tetramethyl-γ-pyrone but contains a small quantity (ca. 5–10%) of 3-methylhex-2-en-4-one. The 3-methylhex-2-ene-4-one does not interfere with the subsequent reaction, and the product was not purified further.

^1H NMR (60 MHz, CCl_4): δ 1.45 (d, 6 H, J = 7 Hz), 1.80 (d, 6 H, J = 7 Hz), 2.60 (m, 2 H), 3.80 (m, 2 H).

2,3,4,5-Tetramethylcyclopent-2-enone. A 12-L three-necked round-bottom reaction flask was cooled in ice. It was charged with 6500 mL of 95–97% HCOOH and 2250 mL of H_2SO_4 and the solution allowed to cool to room temperature. The 2,3,5,6-tetrahydro-2,3,5,6-tetramethyl-γ-pyrone, 1580 g (10.1 mol), was added with stirring to the acid solution at a fast trickle. The reaction solution was then heated to 50 °C and stirred for 16–24 h. The resulting dark brown organic mixture was next poured in 500-mL aliquots into 1000 g of ice. Ether (500 mL) was added and the aqueous phase was removed and back-extracted with 2 × 250 mL of ether. The combined ether layers were washed with 2 × 500 mL of 2 N NaCl and 10% NaOH until the aqueous layer became yellow. The aqueous layer was then checked with pH paper to ensure alkalinity. (Failure to remove all HCOOH from the organic layer results in product decomposition during the final distillation.) The organic layer was again washed with 2 N NaCl and the ether removed by rotary evaporation. The crude product was then purified by fractional distillation using a Vigreux column and water aspirator. The yellow liquid boiling at 77–90 °C (15 Torr) was collected. Yield: 1045 g (75%).

^1H NMR (60 MHz, CCl_4): δ 1.20 (m, 2 H), 1.30 (s, 3 H), 1.45 (s, 3 H), 1.80 (s, 3 H), 2.10 (s, 3 H).

1,2,3,4-Tetramethylcyclopentadiene. A 2000-mL three-necked round-bottom flask fitted with a reflux condenser and a 250-mL addition funnel was charged with 16.8 g (0.443 mol) of $LiAlH_4$. Diethyl ether, 900 mL, was then added to the flask and the mixture cooled to 0 °C. Freshly distilled, colorless, 2,3,4,5-tetramethylcyclopent-2-enone, 210 mL (1.40 mol), was added dropwise to the mixture with stirring over a 1-h period. The mixture was allowed to warm to room temperature and stirred for 8 h. Water, 70 mL, was then added dropwise to hydrolyze the remaining $LiAlH_4$. Solids were coagulated by the dropwise addition of 70 mL of 33% H_2SO_4, and the ether layer was decanted into a 2000-mL separatory funnel. Water and 33% H_2SO_4 were added alternately to the remaining solids in the flask until all solids dissolved. The solution was then back-extracted with Et_2O (3 × 50 mL), and the extracts were combined with the ethereal layer. The dehydration of the alcohol was monitored via GC on a 5% FFAP on Chromosorb W column by monitoring the disappearance of the alcohol.[14] An aliquot, 20 mL, of 33% H_2SO_4 was added to the ether layer in the separatory funnel and shaken for 2 min. The aqueous layer was removed and a GC of the ether layer recorded. This procedure was repeated with 20-mL aliquots of 33% H_2SO_4 until no alcohol could be detected by GC. The ether layer was then washed free of the majority of acid with water and checked via GC for the presence of alcohol. If no alcohol was present, a saturated aqueous solution of potassium carbonate was added until the aqueous layer was strongly alkaline. The aqueous layer was then removed, the combined water wash and aqueous layer were back-extracted with 2 × 250 mL of ether, and the ether layers were combined. Anhydrous potassium carbonate was added to the ether layer in the separatory funnel. After 10 min, the ether layer was then decanted onto anhydrous potassium carbonate in a 2-L flask. Subsequent to filtration, the ether was removed by rotary evaporation leaving a yellow to orange liquid. A small

(7) McIlwrick, C. R.; Phillips, C. S. G. *J. Chem. Phys. E* **1973**, *6*, 1208–1210.
(8) Sekutowski, P. D.; Stucky, G. D. *J. Chem. Educ.* **1976**, *53*, 110.
(9) Schrock, R. R.; Fellmann, J. D. *J. Am. Chem. Soc.* **1978**, *100*, 3359–3370.
(10) Collier, M. R.; Lappert, M. F.; Pearce, R. *J. Chem. Soc., Dalton Trans.* **1973**, 445–451.
(11) Eastham, J. F.; Screttas, C. G. U.S. Patent 3 534 113 (see: *Chem. Abstr.* **1971**, *74*, 3723b).
(12) Fagan, P. J.; Manriquez, J. M.; Maatta, E. A.; Seyam, A. M.; Marks, T. J. *J. Am. Chem. Soc.* **1981**, *103*, 6650–6667.
(13) (a) Burger, U.; Delay, A.; Mazenod, F. *Helv. Chim. Acta* **1974**, *57*, 2106–2111. (b) See also: Kohl, F. X.; Jutzi, P. *J. Organomet. Chem.* **1983**, *243*, 119–121. (c) Fendrick, C. M.; Schertz, L. D.; Mintz, E. A.; Marks, T. J., submitted for publication.

(14) (a) The alcohol elutes more slowly than the tetramethylcyclopentadiene. The tetramethylcyclopentadiene appears initially in the GC as three isomers that isomerize to the 2,3,4,5-tetramethylcyclopentadiene as the workup continues. (b) Operations after the addition of H_2SO_4 must be carried out as rapidly as possible to avoid loss of product from undesirable side reactions.

amount of sodium metal (ca. 0.3 g) was added to the flask and the product purified by trap-to-trap distillation. Yield: 69.7 g (45.8%).

^{1}H NMR (60 MHz, C_6D_6): δ 1.78 (s, 6 H), 1.88 (s, 6 H), 2.60 (s, 1 H). IR (neat, cm^{-1}): 2978 s, 2953 s, 2938 s, 2718 m, 1656 m, 1624 m, 1442 s, 1378 s, 1319 m, 1290 w, 1260 w, 1235 m, 1170 m, 1135 m, 1106 m, 956 w, 891 w, 858 m, 848 sh, 838 sh, 765 w, 688 w, 550 w, 475 m, 458 w.

$Cl_2Si[(CH_3)_4C_5H]_2$ ($Cl_2Si(Cp''H)_2$). A 2000-mL three-necked round-bottomed flask was fitted with a 500-mL addition funnel, a gas inlet, and a mechanical stirrer. Tetrahydrofuran, 1000 mL, was transferred to the flask under dinitrogen flush and cooled to 0 °C. Freshly distilled, colorless $(CH_3)_4C_5H$, 75 mL (0.50 mol) was then syringed into the THF under a dinitrogen flush. With stirring, 309 mL of *n*-butyllithium (1.55 M solution in hexane, 0.48 mol) was added dropwise at 0 °C over a period of 1.5 h. The thick yellow mixture was next stirred 10.5 h, allowing the temperature to slowly rise to room temperature. The mixture was subsequently cooled to −78 °C, and 26.5 mL (0.23 mol) of $SiCl_4$ was added dropwise over a 1-h period. The mixture was warmed slowly to room temperature, and the clear yellow solution was stirred for 2 h. The solvent was removed in vacuo and the resulting solid dried under vacuum for 12 h. The solid was transferred in the glovebox to a 500-mL reaction flask fitted with a Schlenk frit and extracted with pentane (8 × 50 mL). After each addition of pentane, the mixture was filtered through Celite. The filtrate volume was then reduced to ca. 20 mL and cooled to −78 °C which caused it to solidify. Enough pentane was syringed in under dinitrogen flush to form a slurry (about 25 mL), and the colorless solid was collected by filtration at −78 °C, followed by drying in vacuo. Yield: 58.8 g (74.7%).

^{1}H NMR (90 MHz, C_6H_6): δ 1.65 (s, 12 H), 1.95 (s, 12 H), 3.15 (s, 2 H). IR (Nujol, cm^{-1}): 1638 m, 1295 w, 1213 s, 1112 s, 1080 m, 1050 w, 1030 w, 1000 w, 986 w, 956 w, 929 w, 795 w, 780 w, 730 m, 700 m, 563 s, 538 sh, 528 s, 510 s, 500 m, 489 m.

Anal. Calcd for $C_{18}H_{26}Cl_2Si$: C, 63.32; H, 7.68; Cl, 20.77. Found: C, 63.83; H, 7.30; Cl, 20.98.

$(CH_3)_2Si[(CH_3)_4C_5H]_2$ ($Me_2Si(Cp''H)_2$). A 2000-mL three-necked flask fitted with a 500-mL addition funnel, mechanical stirrer, and gas inlet was charged with 32.0 g (0.094 mol) of $Cl_2Si[(CH_3)_4C_5H]_2$. Diethyl ether, 500 mL, was transferred to the reaction flask and the solution cooled to −78 °C. Methyllithium, 235 mL (0.364 mol, 3.9 eq of a 1.55 M solution in Et_2O), was added dropwise over 1.5 h. The reaction mixture was allowed to warm to 0 °C and stirred for 3.5 h. The reaction mixture was then cooled to −78 °C, and 11.6 mL (0.287 mol, 3 equiv) of methanol was slowly syringed into the mixture. When gas evolution had ceased, the reaction was warmed to room temperature. The solvent was next removed in vacuo, and the resulting pale yellow solids were transferred in the glovebox to a 500-mL, round-bottom reaction flask fitted with a Schlenk frit. Pentane (7 × 50 mL) was syringed in under a dinitrogen flush. After each addition, the solution was decanted into the frit and filtered through Celite. The solvent was next removed in vacuo, and the yellow oil was cooled to −78 °C to yield a solid. Pentane (enough to form a slurry) was then syringed in under a dinitrogen flush while the slurry was kept at −78 °C. The solid was collected by filtration at −78 °C and dried in vacuo at room temperature. Yield: 20.5 g (73%).

^{1}H NMR (90 MHz, C_6D_6): δ −0.20 (s, 6 H), 1.82 (s, 12 H), 1.95 (s, 12 H), 3.13 (s, 2 H). IR (Nujol, cm^{-1}): 1632 m, 1400 vw, 1300 w, 1247 s, 1215 m, 1120 w, 1110 w, 1042 m, 1020 m, 983 s, 950 m, 915 sh, 832 m, 811 s, 789 m, 775 m, 723 w, 698 w, 680 w, 639 m.

Anal. Calcd for $C_{20}H_{32}Si$: C, 79.92; H, 10.73. Found: C, 80.50; H, 11.00.

$Me_2SiCp''_2Li_2$·2DME. A 300-mL three-necked round-bottom flask fitted with a gas, inlet magnetic stir bar, and addition funnel was charged with 10.23 g (34.04 mmol) $(CH_3)_2Si[(CH_3)_4C_5H]_2$. Dimethoxyethane, 80 mL, was syringed into the flask. The solution was then cooled to −78 °C, and 44 mL (70.4 mmol) of 1.6 M solution of *n*-BuLi in hexane was added dropwise with stirring over 1 h. The reaction mixture was then warmed to room temperature. During this time the solution changed from yellow to orange in color and a precipitate formed. After the solution was stirred 4 h, the solvent was removed in vacuo. Pentane, 100 mL, and DME, 50 mL, were syringed onto the solids and the solids broken up into a fine powder by stirring. The colorless solid was collected by filtration, washed with 50 mL of pentane, and dried in vacuo overnight. Yield: 13.45 g (80%).

IR (Nujol, cm^{-1}): 1296 m, 1236 m, 1228 sh, 1182 w, 1110 m, 1069 s, 1021 br w, 870 m, 826 sh, 812 s, 748 w, 742 sh, 720 w, 671 m, 656 w, 486 br w, 446 w.

Anal. Calcd for $C_{28}H_{50}SiLi_2O_4$: C, 68.26; H, 10.23. Found: C, 68.66; H, 10.37.

$Me_2SiCp''_2Li_2$·x THF. The $Me_2SiCp''_2Li_2$·*x*THF was synthesized in a manner identical with $Me_2SiCp''_2Li_2$·2DME above using THF, 7.38 g (24.6 mmol) of $(CH_3)_2Si(Cp''H)_2$, and 31.2 mL (49.9 mmol) of 1.6 M solution *n*-BuLi in hexane. Yield: 8.93 g.

IR (Nujol, cm^{-1}): 1330 w, 1300 s, 1248 s, 1190 w, 1133 m, 1050 s, 1014 m, 918 sh, 896 m, 832 s, 820 s, 809 s, 752 m, 680 m, 660 m.

$Me_2SiCp''_2(MgCl·DME)_2$. Isopropylmagnesium chloride, 48 mL (0.14 mol) of a 3.0 M solution in Et_2O, was syringed under a dinitrogen flush into a 250-mL round-bottom flask equipped with a Kontes valve side arm and magnetic stir bar. As much Et_2O as possible was removed in vacuo with the aid of a warm water bath, leaving a white gelatinous material in the flask. Toluene, ca. 40 mL, was then syringed into the flask under a dinitrogen flush. The Kontes valve on the flask was closed, one inlet of an ice-cooled trap was connected to the vacuum valve of the flask, and the other inlet was connected to a vacuum line. The trap was evacuated and back-filled with dinitrogen three times and then the Kontes valve to the flask opened. A toluene solution, 20 mL, containing 19.5 g (65 mmol) of $Me_2Si(Cp''H)_2$ was syringed slowly into the ipsopropylmagnesium chloride suspension under a dinitrogen flush. Excessive frothing was prevented by periodically cooling in an ice bath. When the frothing subsided, the flask was lowered into a 110 °C oil bath. The reaction was removed from the oil bath periodically to prevent violent frothing. As the reaction proceeded, any remaining Et_2O was distilled into the ice-cooled trap. After 30 min, the gas evolution subsided and the suspension was allowed to stir at 110 °C for 4.5 h. The reaction mixture was then cooled to room temperature, and 40 mL of DME was slowly syringed into the reaction mixture. The solids coagulated at the bottom of the flask as an oily mass. After the mass was allowed to stand for 12–15 h, a white crystalline solid formed. The solid was broken up with a spatula and the slurry stirred for 2 h. The colorless solids were then collected by filtration and dried in vacuo. Yield: 35.8 g (92%).

IR (Nujol, cm^{-1}): 1301 s, 1236 m, 1231 sh, 1186 w, 1082 sh, 1042 vs, 977 w, 859 s, 836 sh, 826 vs, 815 sh, 756 w, 664 w, 445 m.

$Me_2SiCp''_2ThCl_2$·2LiCl·2DME (1). A three-necked 250-mL round-bottom flask equipped with a magnetic stir bar was charged with 5.05 g (13.5 mmol) of $ThCl_4$ and 6.72 g (13.6 mmol) of $Me_2SiCp''_2Li_2$·DME Dimethoxyethane, 120 mL, was syringed into the flask under a dinitrogen flush, and the reaction mixture was heated at reflux with stirring for 16 h. Removal of the solvent in vacuo yielded a yellow solid. The solid was transferred in the glovebox to a 100-mL flask fitted with a Schlenk frit, extracted with DME (3 × 40 mL), and filtered. The solvent was next removed in vacuo and the resulting solids washed with 50 mL of pentane. The colorless to pale yellow solid was then dried in vacuo. Yield: 8.62 g (77%).

The sample for elemental analysis was recrystallized from toluene, followed by recrystallization from DME, and dried in vacuo overnight.

^{1}H NMR (90 MHz, $CDCl_3$): δ 0.84 (s, 6 H), 2.06 (s, 12 H), 2.41 (s, 12 H), 3.52 (s, 12 H), 3.58 (s, 8 H). IR (Nujol, cm^{-1}): 1402 w, 1332 w, 1322 sh, 1263 w, 1255 m, 1250 m, 1192 m, 1120 s, 1081 s, 1020 s, 871 s, 838 s, 822 w, 809 s, 764 m, 672 s, 650 w, 572 w, 458 w, 386 w.

Anal. Calcd for $C_{28}H_{50}Cl_4Li_2O_4SiTh$: C, 38.82; H, 5.82; Cl, 16.37; Li, 1.59; Si, 3.24; Th, 26.78; O, 7.58. Found: C, 38.76; H, 5.80; Cl, 16.06; Li, 1.48; Si, 3.19; Th, 26.92; O, 7.79 (by difference).

$Me_2SiCp''_2ThCl_2$·x($MgCl_2$·DME). A 1-L round-bottom flask equipped with a Teflon vacuum valve side arm and a magnetic stir bar was charged with 8.69 g (23.2 mmol) of finely powdered $ThCl_4$ and 14.81 g of $Me_2SiCp''_2$·$(MgCl·DME)_2$ (24.8 mmol). Dimethoxyethane, 350 mL, was added under a helium flush, and the flask was lowered into a 100 °C oil bath and heated with stirring for 48 h. After the heating was complete, the DME was removed in vacuo leaving an oil that crystallized upon standing

overnight. The solids were washed several times with pentane and dried in vacuo. Dimethoxyethane, about 200 mL, was then added to the solid and the mixture filtered. The white solids were washed with 25 mL of DME and the washings filtered and combined with the filtrate. The solvent was next removed in vacuo to yield a colorless solid product. The product was washed with the 50 mL of pentane and dried in vacuo. Yield: 19.6 g.

^{1}H NMR (90 MHz, $CDCl_3$): δ 0.83 (s, 6 H), 2.03 (s, 12 H), 2.39 (s, 12 H), 3.60 (s, $(CH_3OCH_2)_2$), 3.79 (s, $(CH_3OCH_2)_2$). IR (Nujol mull, cm^{-1}): 1405 vw, 1330 w, 1248 m, 1190 m, 1091 br sh, 1052 br s, 1026 sh, 818 s, 847 s, 810 s, 710 n, 670 s, 650 w, 6572 w, 460 m.

$Me_2SiCp''_2Th[CH_2Si(CH_3)_3]_2$ (2a). A two-necked 100-mL round-bottom reaction flask equipped with a magnetic stir bar was charged with 1.78 g (2.16 mmol) of $Me_2SiCp''_2ThCl_2$·2LiCl·2DME. [(Trimethylsilyl)methyl]lithium, 0.43 g (4.57 mmol), was placed in a solid addition tube and the tube attached to the flask. In vacuo at −78 °C, 25 mL of DME was condensed into the flask. The solution was allowed to warm to −10 °C, and the $LiCH_2Si(CH_3)_3$ was added. The reaction mixture was then stirred for 2.5 h between −10 and −30 °C. The solvent was removed in vacuo, and the yellow, gummy solids were dried overnight in vacuo. Pentane, 20 mL, was condensed onto the solids at −78 °C and the mixture warmed to room temperature and filtered. The solid residue was washed with pentane (3 × 15 mL), and the washings were combined with the filtrate. The filtrate volume was next reduced to 10 mL and cooled to −78 °C to precipitate a colorless solid. The solid was collected by filtration at −78 °C. After recrystallization from DME, a colorless solid was obtained. Yield: 0.78 g (51%).

^{1}H NMR (270 MHz, C_6D_6): δ −0.58 (s, 4 H), 0.25 (s, 18 H), 0.72 (s, 6 H), 2.08 (s, 12 H), 2.10 (s, 12 H). ^{13}C NMR (67.80 MHz, C_6D_6): δ 132.62 (s), 129.43 (s), 101.44 (s), 81.52 (t, J_{C-H} = 99 Hz), 14.91 (q, J_{C-H} = 126.5 Hz), 4.43 (q, J_{C-H} = 117.3 Hz), 3.37 (q, J_{C-H} = 119.1 Hz). IR (Nujol mull, cm^{-1}): 2918 s, 2875 sh, 2830 sh, 2720 w, 2704 w, 1441 w, 1405 sh, 1382 w, 1342 w, 1308 m, 1252 m, 1240 s, 1122 br m, 1010 w, 913 w, 850 s, 840 s, 810 s, 808 s, 770 m, 750 m, 728 m, 710 m, 680 m, 460 m, 380 w.

Anal. Calcd for $C_{28}H_{52}Si_3Th$: C, 47.76; H, 7.43. Found: C, 47.86; H, 7.53.

$Me_2SiCp''_2Th[CH_2C(CH_3)_3]_2$ (2b). A 30-mL two-necked flask equipped with a magnetic stir bar was charged with 0.94 g (1.14 mmol) of $Me_2SiCp''_2ThCl_2$·2LiCl·2DME. A solid addition tube containing 0.19 g (2.43 mmol) of neopentyllithium was attached to the flask. In vacuo at −78 °C, 15 mL of DME was condensed into the flask. The mixture was warmed to −40 °C, and the neopentyllithium was slowly added. The reaction was then warmed to −20 °C and stirred for 2 h. The solvent was removed in vacuo at −10 °C and the yellow solid was dried in vacuo at −78 °C overnight. Heptane, 15 mL, was condensed onto the solids. The mixture was stirred and filtered. The yellow tar that remained in the flask was washed twice with 10 mL of heptane, and the washings were combined with the filtrate. The solvent was then removed in vacuo, and the yellow solids were recrystallized from DME to give a colorless solid. Yield: 0.29 g (38%).

^{1}H NMR (90 MHz, C_6D_6): δ 0.10 (s, 4 H), 0.76 (s, 6 H), 1.22 (s, 18 H), 2.11 (s, 12 H), 2.16 (s, 12 H). IR (Nujol mull, cm^{-1}): 2622 w, 1353 m, 1304 s, 1257 sh, 1232 m, 1203 m, 1102 br m, 1010 br m, 989 sh, 940 w, 905 w, 840 s, 812 sh, 810 s, 761 w, 749 w, 735 w, 660 m, 652 w, 620 m, 504 w, 450 s.

Anal. Calcd for $C_{30}H_{52}SiTh$: C, 53.55; H, 7.79; Th, 34.48. Found: C, 53.58; H, 7.54; Th, 34.68.

$Me_2SiCp''_2Th(C_6H_5)_2$ (2c). Phenyllithium, 0.48 mL (1.30 mmol) of a 2.7 M solution in cyclohexane/Et_2O, was syringed into a two-necked 30-mL flask under a helium flush and the solvent removed in vacuo. The flask was then charged with 0.50 g (0.61 mmol) of $Me_2SiCp''_2ThCl_2$·2LiCl·2DME. In vacuo at −78 °C, 15 mL of DME was condensed into the flask and the reaction mixture warmed to 0 °C. The resulting brown solution was stirred for 5 h at 0 °C and the solvent removed in vacuo. Benzene, 10 mL, was condensed onto the solids, and the mixture was stirred at room temperature and filtered to yield a light brown filtrate. The solids were washed twice with 5-mL portions of benzene and the washings combined with the filtrate. The benzene was then removed under high vacuum to yield a pink solid. Recrystallization from pentane yielded a colorless solid. Yield: 0.06 g (15%).

^{1}H NMR (90 MHz, C_6D_6): δ 0.87 (s, 6 H), 1.65 (s, 12 H), 2.32 (s, 12 H), 7.09–7.65 (m, 10 H). IR (Nujol mull, cm^{-1}): 1410 w, 1340 w, 1300 m, 1210 m, 1198 sh, 1056 sh, 1038 s, 1010 s, 989 w, 836 m, 808 s, 762 w, 692 m, 631 w, 621 m, 458 m.

Anal. Calcd for $C_{32}H_{40}SiTh$: C, 56.13; H, 5.89. Found: C, 56.15; H, 5.98.

$Me_2SiCp''_2Th(n\text{-}C_4H_9)_2$ (2d). Under an argon flush, 3.20 mL (5.12 mmol) of 1.6 M *n*-BuLi solution in hexane was syringed into a 50-mL, two-necked flask equipped with a magnetic stir bar, and the hexane was removed in vacuo. Two grams (2.43 mol) of $Me_2SiCp''_2ThCl_2$·2LiCl·2DME was placed in a solid addition tube and the tube attached to the flask. Dimethoxyethane, 25 mL, was condensed onto the *n*-BuLi at −78 °C. The solution was warmed to −30 °C, and the $Me_2SiCp''_2ThCl_2$·2LiCl·2DME was added slowly. The mixture was stirred 5 min, then warmed to −15 °C, and stirred for 1 h. The reaction was then warmed to 0 °C and stirred 0.5 h more. The DME was removed in vacuo at 0 °C to yield a yellow oil. Pentane, 20 mL, was condensed onto the oil at −78 °C, and the mixture was allowed to warm to room temperature. The pentane was then removed in vacuo, and the orange-brown solids were dried in vacuo 13 h. Pentane, 30 mL, was condensed onto the solids and the mixture filtered. The orange gummy solids were washed twice with 15 mL of pentane and the washings combined with the pale yellow filtrate. The volume of the solution was next reduced to 10 mL and the solution slowly cooled to −78 °C. The resulting solid was collected via cold filtration. Recrystallization from DME gave a pale yellow solid. Yield: 0.66 g (42%).

^{1}H NMR (90 MHz, C_6D_6): δ 0.09 (t, 4 H), 0.78 (s, 6 H), 1.06 (t, 6 H), 1.45 (m, 8 H), 1.97 (s, 12 H), 2.17 (s, 12 H). IR (Nujol mull, cm^{-1}): 1405 w, 1342 m, 1247 s, 1168 w, 1144 w, 1122 w, 1092 w, 1052 w, 1042 w, 1008 br m, 957 w, 932 w, 842 m, 837 sh, 812 s, 767 s, 750 w, 747 w, 721 w, 678 m, 755 w, 493 sh, 452 s.

Anal. Calcd for $C_{28}H_{48}SiTh$: C, 52.16; H, 7.50. Found: C, 52.20; H, 7.39.

$Me_2SiCp''_2Th(CH_2C_6H_5)_2$ (2e). A 100-mL two-necked flask equipped with a magnetic stir bar was charged with 2.03 g (2.46 mmol) of $Me_2SiCp''_2ThCl_2$·2LiCl·2DME. Benzyllithium–0.5-tetrahydrofuran, 0.71 g (5.26 mmol), was placed in a solid addition tube and the tube attached to the flask. Dimethoxyethane, 20 mL, was condensed into the flask at −78 °C. The $Me_2SiCp''_2ThCl_2$·2LiCl·2DME was dissolved by warming the mixture to room temperature, and then the solution was cooled to 0 °C. The benzyllithium was added, and the orange solution was stirred for 1.5 h at 0 °C. The solvent was then removed in vacuo, and the orange solids were dried in vacuo overnight. Toluene (50 mL) was next condensed onto the solids and the orange mixture filtered. The solids on the frit were washed twice with 20 mL of toluene and the washings combined with the filtrate. The filtrate volume was then reduced to 5 mL, and 20 mL of pentane was condensed into the flask. The resulting light orange solid was collected by filtration. Recrystallization from a mixture of 1:1 toluene/pentane afforded a yellow solid. Yield: 0.46 g (26%).

^{1}H NMR (90 MHz, C_6D_6): δ 0.72 (s, 6 H), 0.95 (s, 4 H), 1.78 (s, 12 H), 2.10 (s, 12 H), 6.45–7.22 (m, 10 H). IR (Nujol mull, cm^{-1}): 1591 s, 1405 w, 1348 w, 1307 s, 1251 s, 1211 s, 1174 m, 1158 w, 1147 w, 1124 w, 1106 w, 1072 w, 1011 m, 991 w, 962 s, 953 s, 894 m, 878 w, 831 s, 809 s, 800 s, 772 w, 742 s, 728 w, 702 s, 678 m, 653 w, 537 w, 548 w, 512 w, 504 w, 452 s, 382 w.

Anal. Calcd for $C_{34}H_{44}SiTh$: C, 57.29; H, 6.22. Found: C, 57.27; H, 6.26.

Reaction of $Me_2SiCp''_2ThCl_2$·2DME·2LiCl and MeLi. A 50-mL two-necked flask equipped with a magnetic stir bar was charged with 1.8 mL (2.5 mmol) of 1.4 M MeLi solution in Et_2O under an argon flush. The Et_2O was next removed in vacuo. An addition tube containing 0.50 g (0.61 mmol) of $Me_2SiCp''_2ThCl_2$·2DME·2LiCl was attached to the flask. DME (15 mL) was condensed into the flask at −78 °C, the mixture warmed to −30 °C, and the $Me_2SiCp''_2ThCl_2$·2DME·2LiCl added. The mixture was then stirred for 2 h between −30 and −10 °C, during which time the color became light brown. The DME was next removed in vacuo and the resulting solid washed with pentane. This material decomposes upon attempted dissolution in toluene. The general procedure was also followed by using 2–4 equiv of MeLi. The order of addition of MeLi and

$Me_2SiCp''_2ThCl_2 \cdot 2DME \cdot 2LiCl$ was also reversed in some experiments.

$(Me_2SiCp''_2ThH_2)_2$ (3). A 30-mL flask equipped with a magnetic stir bar was charged with 0.83 g (1.18 mmol) of $Me_2SiCp''_2Th[CH_2Si(CH_3)_3]_2$. Pentane, 15 mL, was condensed onto the solids at −78 °C and the reaction warmed to room temperature to dissolve the solids. After the flask was wrapped in aluminum foil, the solution was placed under 1 atm of hydrogen and stirred for 8 h. The resulting lemon-yellow precipitate was collected by filtration, washed with pentane (3 × 15 mL), and dried in vacuo. Yield: 0.56 g (90%).

^1H NMR (270 MHz, C_6D_6): δ 0.79 (s, 12 H), 2.32 (s, 24 H), 2.39 (s, 24 H), 18.36 (s, 4 H). IR (cm^{-1}): 1442 m, 1402 w, 1380 m, 1315 w, 1285 v br, 1256 m, 1250 m, 1155 w, 1010 w, 940 w, 833 m, 810 s, 752 m, 750 m, 680 s, 654 m, 645 m, 570 w, 481 w, 458 m.

Anal. Calcd for $C_{40}H_{64}Si_2Th_2$: C, 45.10; H, 6.06. Found: C, 45.14; H, 6.10.

$(Me_2SiCp''_2ThD_2)_2$ (3-*d*). The compound $(Me_2SiCp''_2ThD_2)_2$ was prepared in a manner identical with that of $(Me_2SiCp''_2ThH_2)_2$ by using 0.27 g (0.38 mmol) of $Me_2SiCp''_2Th[CH_2Si(CH_3)_3]_2$ and deuterium gas. Yield: 0.17 g (85%).

^1H NMR (90 MHz, C_6D_6): δ 0.79 (s, 12 H), 2.32 (s, 24 H), 2.39 (s, 24 H). IR (cm^{-1}): 1442 m, 1402 w, 1380 m, 1310 s, 1260 m, 1252 s, 1013 m, 953 br m, 918 br m, 835 m, 811 s, 760 w, 750 w, 673 s, 462 s.

Catalytic Hydrogenation of 1-Hexene and *trans*-2-Hexene. Rates of olefin hydrogenation catalyzed by $(Cp'_2ThH_2)_2$ and $(Me_2SiCp''_2ThH_2)_2$ were measured via hydrogen uptake either using simple vacuum line/mercury manometer techniques[12] or using the constant volume, pseudoconstant pressure/vortex mixer apparatus described previously.[15] The latter procedure was necessary when catalytic rates were rapid enough to be influenced by mass transport effects (hydrogen starvation). Thus, while for 1-hexene/$(Cp'_2ThH_2)_2$, *trans*-2-hexene/$(Cp'_2ThH_2)_2$, and *trans*-2-hexene/$(Me_2SiCp''_2ThH_2)_2$, measured rates of hydrogen uptake were identical by both procedures, the 1-hexene/$(Me_2SiCp''_2ThH_2)_2$ system could only be studied by the second approach.

X-ray Crystallographic Studies[16] of $(CH_3)_2Si[(CH_3)_4C_5]_2Th[CH_2Si(CH_3)_3]_2$ (2a) and $\{(CH_3)_2Si[(CH_3)_4C_5]_2ThH_2\}_2$ (3). Well-shaped pale yellow single crystals of $Me_2SiCp''_2Th[CH_2Si(CH_3)_3]_2$ (**2a**) obtained by slow cooling of a saturated pentane solution are, at 20 ± 1 °C, monoclinic, space group $P2_1/m$—C^2_{2h} (No. 11)[17a] with a = 11.960 (5) Å, b = 11.270 (5) Å, c = 12.395 (6) Å, β = 99.32 (4)°, and Z = 2 [μ_a(Mo K$\bar{\alpha}$)[18a] = 4.80 mm^{-1}; d_{calcd} = 1.422 g cm^{-3}]. Well-shaped yellow single crystals of $[Me_2SiCp''_2ThH_2]_2$ (**3**) suitable for X-ray diffraction studies were obtained by slow diffusion of hydrogen into a heptane solution of **2a**. They are, a 20 ± 1 °C, monoclinic, space group $P2_1/n$ [an alternate setting of $P2_1/c$—C^5_{2h} (No. 14)[17b]] with a = 10.965 (2) Å, b = 19.843 (5) Å, c = 18.759 (3) Å, β = 90.39 (2)°, and Z = 4 dimeric units [μ_a(Mo K$\bar{\alpha}$)[18a] = 7.62 mm^{-1}; d_{calcd} = 1.74 g cm^{-3}].

Intensity measurements were made for both compounds on a computer-controlled Nicolet P$\bar{1}$ autodiffractometer using 0.90° wide ω scans and graphite-monochromated Mo K$\bar{\alpha}$ radiation. The samples of **2a** and **3** used in this study were cut under a nitrogen atmosphere with a razor blade from larger single crystals and were glued with epoxy to the inside of a sealed, thin-walled glass capillary. Both samples were rectangular parallelepipeds of dimensions 0.20 × 0.25 × 0.52 mm for **2a** and 0.22 × 0.28 × 0.40 mm for **3**. Both crystals were mounted on the goniometer head with their longest edge nearly parallel to the phi axis of the X-ray diffractometer. A total of 3989 (**2a**) and 7468 (**3**) independent reflections having $2\theta_{MoK\bar{\alpha}} < 55°$ (**2a**) and $2\theta_{MoK\bar{\alpha}} < 50.7°$ (**3**) were measured for both compounds in two concentric shells of increasing 2θ. Scanning rates of 6°/min were employed with both compounds for reflections having $0° < 2\theta_{MoK\bar{\alpha}} < 43°$ and 3°/min

Scheme I

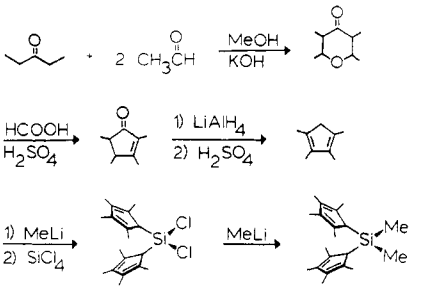

or 4°/min for the remaining reflections. The data collection techniques are described elsewhere;[19] the ratio of background counting time to net peak counting time for the present studies was 0.50. The intensity data for both compounds were corrected empirically for variable absorption effects using psi scans for seven (**2a**) and six (**3**) intense reflections having 2θ between 6.9° and 34.8° for **2a** and 6.1° and 31.6° for **3**, respectively, before reducing them to a set of relative squared amplitudes, $|F_o|^2$, by means of standard Lorentz and polarization corrections.

The metal atoms of both compounds were located from Patterson syntheses and the remaining non-hydrogen atoms from difference Fourier syntheses using progressively more complete structural models. Counter-weighted[19] anisotropic full-matrix least-squares refinement of the structural parameters for the Th and Si atoms of both compounds refined to R_1 (unweighted, based on F)[20] values of 0.144 (**2a**) and 0.138 (**3**) for 2586 (**2a**) and 3298 (**3**) independent absorption-corrected reflections having $I > 3\sigma(I)$. The final cycles[16] of counter-weighted cascade block-diagonal least-squares refinement that employed anisotropic thermal parameters for all non-hydrogen atoms of **2a** gave R_1 = 0.076 and R_2 (weighted, based on F)[20] = 0.075 for 2586 independent absorption-corrected reflections of **2a** having $2\theta_{MoK\bar{\alpha}} < 55°$ and $I > 3\sigma(I)$. The final cycles[16] of counter-weighted cascade block-diagonal least-squares refinement that utilized anisotropic thermal parameters for the Th and Si atoms and isotropic thermal parameters for all carbon atoms gave R_1 = 0.075 and R_2 = 0.082 for 3298 independent absorption-corrected reflections of **3** having $2\theta_{MoK\bar{\alpha}} < 50.7°$ and $I > 3\sigma(I)$.

When all non-hydrogen atoms of **3** had been located and refined, the coordinates for the two halves of the dimer appeared to be related by rigorous crystallographic symmetry; the apparent symmetry operations relating the two halves of the dimer in the monoclinic unit cell were those of the uniquely determined orthorhombic space group *Pbna* (an alternate setting of *Pbcn*—D^{14}_{2h}, No. 60[17c]). With the observed β value of 90.39 (2)° for the monoclinic unit cell and approximate C_s—m symmetry for axial photographs perpendicular to the $\vec{a}^*$ and $\vec{c}^*$ axes of the monoclinic unit cell as well as rigorous C_s—m symmetry perpendicular to the $\vec{b}$ axis, it was decided to pursue structure refinement in the orthorhombic space group *Pbna*. Counter-weighted full-matrix least-squares refinement of **3** (with anisotropic Th and Si atoms and isotropic C atoms) in this space group resulted in R_1 = 0.180 for 3298 independent absorption-corrected reflections having $2\theta_{MoK\bar{\alpha}} < 50.7°$ and $I > 3\sigma(I)$ and unreasonable metrical parameters for many of the ligand non-hydrogen atoms. It was therefore assumed that single crystals of **3** utilize the monoclinic space group $P2_1/n$ to pack dimeric units in a pseudoorthorhombic fashion.

All structure factor calculations for both compounds employed recent tabulations of atomic form factors[18b] and an anomalous dispersion correction[18c] to the scattering factors of the Th and Si atoms. The final cycles of least-squares refinement for both compounds employed a least-squares refinable extinction correction of the form $(1 + 0.002(x)F_c^2 \sin^{-1}(2\theta))^{-1/4}$. All calculations were performed on a Data General Eclipse S-200 or S-230 computer with 256K of 16-bit words, a floating point processor for 32- and 64-bit arithmetic, and versions of the Nicolet E-XTL and

(15) Jeske, G.; Lauke, H.; Mauermann, H.; Schumann, H.; Marks, T. J. *J. Am. Chem. Soc.* **1985**, *107*, 8111–8118.

(16) See paragraph at end regarding supplementary material.

(17) (a) *International Tables for X-ray Crystallography*; Kynoch: Birmingham, England, 1969; Vol. I, p 93. (b) *Ibid.*, p 99. (c) *Ibid.*, p 149.

(18) (a) *International Tables for X-ray Crystallography*; Kynoch: Birmingham, England, 1974; Vol. IV, pp 55–66. (b) *Ibid.*, pp 99–101. (c) *Ibid.*, pp 149–150.

(19) Fagan, P. J.; Manriquez, J. M.; Marks, T. J.; Day, C. S.; Vollmer, S. H.; Day, V. W. *Organometallics* **1982**, *1*, 170–180.

(20) The R values are defined as $R_1 = \sum||F_o| - |F_c||/\sum|F_o|$ and $R_2 = \{\sum w(|F_o| - |F_c|)^2/\sum w|F_o|^2\}^{1/2}$, where w is the weight given each reflection. The function minimized is $\sum w(|F_o| - K|F_c|)^2$ where K is the scale factor.

SHELXTL interactive crystallographic software packages as modified at Crystalytics Co.

Results and Discussion

Ligand Synthesis. The preparation of the ligand $Me_2Si(Cp''H)_2$ is outlined in Scheme I. The precursor 2,3,4,5-tetramethylcyclopent-2-enone was prepared by a modification of the approach of Burger, Delay, and Mazenod.[13] This involves the base-catalyzed condensation of 3-pentanone with acetaldehyde, followed by dehydration of the resulting γ-pyrone (see Experimental Section for details). Reduction of the cyclopentenone with $LiAlH_4$ followed by dehydration of the resulting pentenol yields slightly air-sensitive 2,3,4,5-tetramethylcyclopentadiene ($Cp''H$). Conversion to the lithium salt and reaction with $SiCl_4$ affords air-sensitive, crystalline $Cl_2Si(Cp''H)_2$. Subsequent methylation with CH_3Li and methanol workup yields air-sensitive, crystalline $Me_2Si(Cp''H)_2$. The reagent $Me_2Si(Cp''Li)_2$ is formed by treatment with *n*-BuLi in THF or DME and is isolated as solid THF or DME adducts from these solutions. The Grignard reagent $Me_2SiCp''_2(MgCl\cdot DME)_2$ can be similarly prepared from $Me_2Si(Cp''H)_2$ and *i*-PrMgCl in DME.

Synthesis and Properties of Organothorium Hydrocarbyls. Organothorium halo complex **1**, the precursor to all hydrocarbyls and hydrides, can be prepared via eq 1. The ^1H NMR indicates 2DME/Th, and the stoi-

$$Me_2SiCp''_2Li_2\cdot 2DME + ThCl_4 \xrightarrow{DME} \underset{\mathbf{1}}{Me_2SiCp''_2ThCl_2\cdot 2LiCl\cdot 2DME} \quad (1)$$

chiometry is confirmed by complete elemental analysis. The analogous magnesium reagent $Me_2SiCp''_2ThCl_2\cdot xMgCl\cdot yDME$ can be prepared by reaction of the ligand Grignard reagent with $ThCl_4$ in refluxing DME. Although dioxane is generally useful for removing $MgCl_2$ from organo-f-element complexes,[21] this methodology fails in the present case. The presence of $MgCl_2$ interferes with subsequent thorium alkylation reactions, and this complex was not investigated further. The above observations contrast with Cp'_2ThCl_2 chemistry[12] and suggest a more coordinatively unsaturated thorium environment as well as significant stability for anionic $Me_2SiCp''_2ThCl_n^{2-n}$ species (cf. related lanthanide chemistry[2c,15,22,23]).

Complex **1** undergoes reaction with a variety of lithium reagents to yield the corresponding, thermally stable, colorless to pale yellow bis(hydrocarbyls) (eq 2). The new

$$\mathbf{1} + 2RLi \xrightarrow[DME]{-30\ ^\circ C} \underset{\mathbf{2a-e}}{Me_2SiCp''_2ThR_2} + 4LiCl \quad (2)$$

2a, R = $CH_2Si(CH_3)_3$; **2b**, R = $CH_2C(CH_3)_3$; **2c**, R = C_6H_5; **2d**, R = *n*-C_4H_9; **2e**, R = $CH_2C_6H_5$

complexes were characterized by standard analytical and spectroscopic techniques (see Experimental Section for details). In addition, flame tests indicated the absence of significant quantities of lithium in these compounds. Attempts to prepare an analogous methyl derivative led to a pentane-insoluble material that decomposed in toluene. The ^1H NMR spectrum in THF-d_8 was consistent with the formulation $Me_2SiCp''_2Th(CH_3)_3^-\cdot xDME$. The Th-$CH_3$ ^1H resonance at +1.0 ppm undergoes exchange with added CH_3Li that is rapid on the NMR time scale

Table I. Metal-Hydride Vibrational Modes for Actinide, Lanthanide, and Early-Transition Metal Hydrides

compd	ν_{M-H} (ν_{M-D}), cm^{-1}	ref
$[Me_2SiCp''_2ThH_2]_2$	1285 (918)	this work
	1155	
	654 (462)	
	481	
$[Cp'_2Th(\mu\text{-}H)H]_2$	1404[a] (1002)	12
	1370[a] (979)	
	1215 (873)	
	1114 (609)	
	650 (465)	
$[Cp'_2U(\mu\text{-}H)H]_2$	1335[a]	12
	1180	
$\{[(CH_3)_3Si]_2N\}_3ThH$	1480[a] (1060)	27
$\{[(CH_3)_3Si]_2N\}_3UH$	1430[a] (1020)	28
$Cp'_2Th(OCH_2\text{-}t\text{-}Bu)H$	1355[a] (971)	28
$Cp'_2Th(O\text{-}t\text{-}Bu)H$	1359[a] (981)	12
$[Cp'_2Th(\mu\text{-}H)Cl]_2$	1224	12
	1152	
	859	
	672	
$[Cp'_2La(\mu\text{-}H)]_2$	1120 (800)	22
	940 (660)	
	750 (ca. 510)	
Cp'_2TiH_2	1560[a]	29
Cp'_2ZrH_2	1555[a] (1100)	30
$[C_5H_4(CH_2)_4Zr(\mu\text{-}H)H]_2$	1545[a]	31
	1285	

[a] Assigned to a mode which is predominantly terminal M-H stretching in character.

above room temperature. Although the thermal properties were not investigated in depth, thermolysis of either **2a** or **2b** in cyclohexane-d_{12} at 60 °C does not result in clean cyclometalation to a thoracyclobutane (cf. the Cp'_2ThR_2 analogues[24]). While free neopentane and TMS are detected in the ^1H NMR, an extremely complex pattern is observed in the Cp'' region. Similar results are obtained upon thermolyzing **2b** in benzene or benzene-d_6, and the corresponding diphenyl compound is not observed (in contrast to the analogous Cp'_2ThR_2 system[24,25]).

Synthesis and Properties of a Ring-Bridged Thorium Hydride. The reaction of $Me_2SiCp''_2Th[CH_2Si(CH_3)_3]_2$ with dihydrogen proceeds rapidly in pentane solution to yield the air-sensitive, lemon-yellow hydride **3** (eq 3). With D_2 the corresponding deuteride **3**-*d* is obtained

$$2Me_2SiCp''_2Th[CH_2Si(CH_3)_3]_2 + 4H_2 \rightarrow \underset{\mathbf{3}}{[Me_2SiCp''_2ThH_2]_2} + 4TMS \quad (3)$$

(eq 4). Complex **3** is stable in benzene or toluene solutions

$$2Me_2SiCp''_2Th[CH_2Si(CH_3)_3]_2 + 4D_2 \rightarrow \underset{\mathbf{3}\text{-}d}{[Me_2SiCp''_2ThD_2]_2} + 4TMS\text{-}d_1 \quad (4)$$

for long periods of time in the dark but decomposes in light over the course of several hours to yield a violet solution. The ^1H NMR of **3** is consistent with the $(Me_2SiCp''_2ThH_2)_n$ formulation; the Th-H chemical shift of 18.36 ppm can be compared to that of 19.20 ppm in $(Cp'_2ThH_2)_2$.[12] The low field position is characteristic of d^0 and f^0 hydrides.[2]

Complete infrared spectroscopic data for **3** and **3**-*d* are given in the Experimental Section. Th-H/Th-D modes can be identified by subtracting $Me_2SiCp''_2$-centered transitions deduced from the free ligand and alkyl complexes. Thus, bands at ca. 1440, 1380, 1300, and 1250 cm^{-1}

(21) Mintz, E. A.; Moloy, K. G.; Marks, T. J.; Day, V. W. *J. Am. Chem. Soc.* **1982**, *104*, 4692–4695.
(22) Jeske, G.; Lauke, H.; Mauermann, H.; Swepston, P. N.; Schumann, H.; Marks, T. J. *J. Am. Chem. Soc.* **1985**, *107*, 8091–8103.
(23) (a) Schumann, H. In ref 2c, Chapter 2. (b) Evans, W. J. *Adv. Organomet. Chem.* **1985**, *24*, 131–177. (c) Watson, P. L.; Parshall, G. W. *Acc. Chem. Res.* **1985**, *18*, 51–56.
(24) Bruno, J. W.; Smith, G. M.; Marks, T. J.; Fair, C. K.; Schultz, A. J.; Williams, J. M. *J. Am. Chem. Soc.* **1986**, *108*, 40–56.
(25) Fendrick, C. M.; Marks, T. J. *J. Am. Chem. Soc.* **1986**, *108*, 425–437.

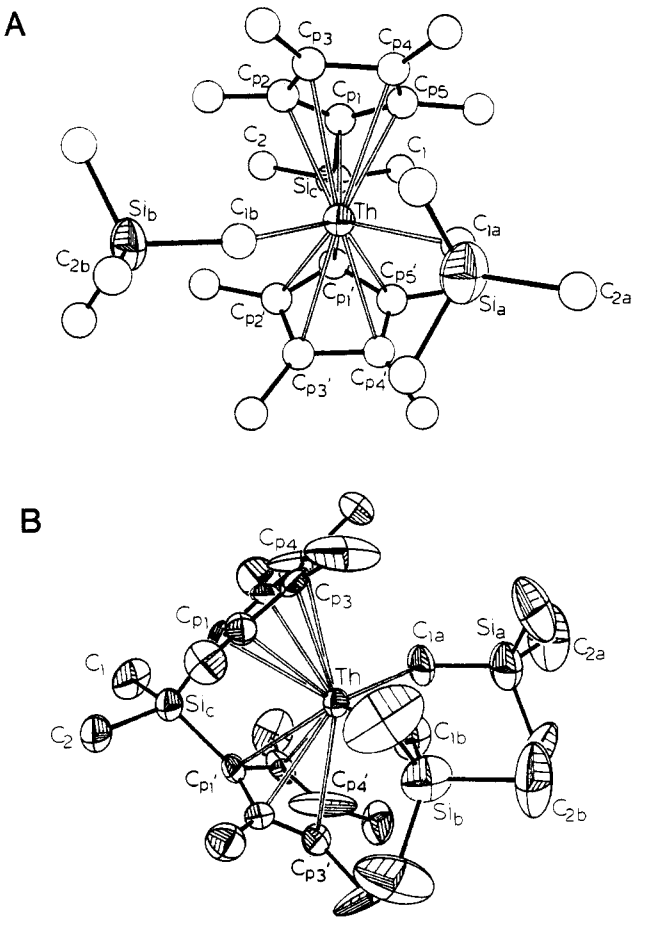

Figure 1. Two views of the molecular structure of $(CH_3)_2Si[(CH_3)_4C_5]_2Th[CH_2Si(CH_3)_3]_2$ (**2a**). Thermal vibrational ellipsoids are drawn to encompass 50% of the electron density. Atoms denoted by a prime are related to those without a prime by the crystallographic mirror plane at (x, $^1/_4$, z). For clarity, methyl carbon atoms C_{3a}, C_{3a}' and C_{3b}, C_{3b}', attached to Si_a and Si_b, respectively, are left unlabeled.

are assignable to Si–CH_3 deformations and those at ca. 840 cm^{-1} to CH_3 rocking/Si–C stretching modes.[6,26] The absorptions at 1010 and 680 cm^{-1} appear to be Cp″-centered.[26] Comparison of the spectra of **3** and **3-*d*** then yields Th–H- (Th–D-) centered modes at 1285 s, br (918, $\nu_{Th-H/Th-D}$ = 1.40), 1155 w (819 calcd), 654 m (462 s, $\nu_{Th-H/Th-D}$ = 1.42), and 481 w cm^{-1} (341 calcd). These data are compared to results for analogous actinide,[12,27,28] lanthanide,[22] and early-transition-metal hydrides in Table I. Most noteworthy is the absence in **3** of detectable bands in the region usually assigned to terminal M–H stretching modes (≥1300–1350 cm^{-1}). For example $(Cp'_2ThH_2)_2$, shown to have structure B by neutron diffraction,[32] exhibits prominent Th–H modes at 1404 and 1370 cm^{-1}. Such transitions are not evident in **3**, strongly suggesting

(26) (a) Smith, A. L. *Spectrochim. Acta* **1960**, *16*, 87–105. (b) Maslowsky, D., Jr. *Vibrational Spectra of Organometallic Compounds*; Wiley: New York, 1977; pp 65–72.
(27) Turner, H. W.; Simpson, S. J.; Andersen, R. A. *J. Am. Chem. Soc.* **1979**, *101*, 2782.
(28) Moloy, K. G.; Marks, T. J. *J. Am. Chem. Soc.* **1984**, *106*, 7051–7064.
(29) Bercaw, J. E.; Marvich, R. H.; Bell, L. G.; Britzinger, H. H. *J. Am. Chem. Soc.* **1972**, *94*, 1219–1238.
(30) Bercaw, J. E. *Adv. Chem. Ser.* **1978**, *No. 167*, 136–148.
(31) Weigold, H.; Bell, A. P.; Willing, R. I. *J. Organometal. Chem.* **1974**, *73*, C23–C24.
(32) Broach, R. W.; Schultz, A. J.; Williams, J. M.; Brown, G. M.; Manriquez, J. M.; Fagan, P. J.; Marks, T. J. *Science (Washington, D.C.)* **1979**, *203*, 172–174.

Table II. Atomic Coordinates for Non-Hydrogen Atoms in Crystalline $(CH_3)_2Si[\eta^5-(CH_3)_4C_5]_2Th[CH_2Si(CH_3)_3]_2$ (2a)[a]

atom type[b]	fractional coordinates 10^3x	10^3y	10^3z	equivalent isotropic thermal parameters, B,[d] Å^2
Th	229.9 (1)	250.0 (...)[c]	296.3 (1)	2.6 (1)
Si_b	287.8 (7)	250.0 (...)[c]	−31.3 (7)	5.4 (3)
Si_a	−91.1 (6)	250.0 (...)[c]	191.2 (8)	6.1 (3)
Si_c	453.6 (5)	250.0 (...)[c]	512.3 (6)	3.4 (3)
C_1	451 (2)	250 (...)[c]	665 (2)	5.6 (9)
C_2 (2)	607 (2)	250 (...)[c]	506 (2)	4.8 (8)
C_{1a}	20 (2)	250 (...)[c]	309 (2)	4.6 (8)
C_{2a}	−240 (2)	250 (...)[c]	229 (3)	10.3 (16)
C_{3a}	−84 (2)	387 (2)	103 (2)	9.7 (10)
C_{1b}	216 (2)	250 (...)[c]	94 (2)	4.4 (8)
C_{2b}	167 (3)	250 (...)[c]	−154 (3)	9.2 (14)
C_{3b}	375 (2)	387 (2)	−43 (2)	10.1 (11)
C_{p1}	374 (1)	379 (1)	439 (1)	3.2 (4)
C_{p2}	389 (1)	426 (1)	335 (1)	3.1 (4)
C_{p3}	299 (1)	494 (1)	294 (1)	3.8 (5)
C_{p4}	220 (2)	490 (1)	383 (2)	7.2 (9)
C_{p5}	263 (1)	422 (1)	453 (2)	4.6 (6)
C_{m2}	492 (1)	414 (1)	283 (1)	4.8 (6)
C_{m3}	273 (2)	566 (1)	180 (1)	8.5 (9)
C_{m4}	110 (1)	564 (1)	360 (2)	6.0 (7)
C_{m5}	209 (2)	409 (2)	561 (2)	6.2 (7)

[a] Numbers in parentheses are the estimated standard deviations in the last significant digit. [b] Atoms are labeled in agreement with Figure 1. [c] This is a symmetry-required value and is therefore listed without an estimated standard deviation. [d] This is one-third of the trace of the orthogonalized $\mathbf{B}_{ij}$ tensor.

Table IV. Bond Lengths (Å) and Angles (deg) Involving Non-Hydrogen Atoms in Crystalline $(CH_3)_2Si[\eta^5-(CH_3)_4C_5]_2Th[CH_2Si(CH_3)_3]_2$ (2a)[a]

parameter[b]	value	parameter[b]	value
	Bond Lengths		
Th–C_{1a}	2.542 (22)	Si_a–C_{3a}	1.898 (27)
Th–C_{1b}	2.481 (24)	Si_a–C_{2a}	1.917 (32)
Th–Cp_1	2.686 (14)	Si_b–C_{3b}	1.875 (26)
Th–Cp_2	2.744 (13)	Th–Si_c	3.465 (6)
Th–Cp_3	2.875 (13)	Cp_1–Cp_5	1.448 (21)
Th–Cp_4	2.917 (17)	Cp_1–Cp_2	1.442 (23)
Th–Cp_5	2.733 (19)	Cp_2–Cp_3	1.357 (20)
Si_c–Cp_1	1.882 (14)	Cp_3–Cp_4	1.555 (32)
Si_c–C_1	1.901 (27)	Cp_4–Cp_5	1.211 (27)
Si_c–C_2	1.849 (25)	Cp_2–C_{m2}[c]	1.480 (24)
Si_a–C_{1a}	1.805 (24)	Cp_3–C_{m3}[c]	1.611 (24)
Si_b–C_{1b}	1.899 (28)	Cp_4–C_{m4}[c]	1.546 (27)
Si_a–C_{2a}	1.913 (34)	Cp_5–C_{m5}[c]	1.589 (31)
	Bond Angles		
Th–C_{1a}–Si_a	123.7 (14)	Cp_1–Si_c–Cp'_1	100.6 (9)
Th–C_{1b}–Si_b	149.5 (12)	C_g–Th–C_g'[d]	118.4 (...)
C_{1a}–Th–C_{1b}	98.9 (8)	C_g–Th–C_{1a}[d]	106.4 (...)
C_1–Si_c–C_2	102.7 (13)	C_g–Th–C_{1b}[d]	112.2 (...)

[a] Numbers in parentheses are the estimated standard deviation in the last significant digits. [b] Atoms are labeled in agreement with Tables II and III and Figure 1. [c] C_{mx} labels refer to methyl groups on ring carbons Cp_x. [d] C_g and C_g' designate the centers-of-gravity for the five-membered rings of the two $(CH_3)_4C_5$ ligands.

an all-bridged structure (C). The proposal is supported by the diffraction results (vide infra).

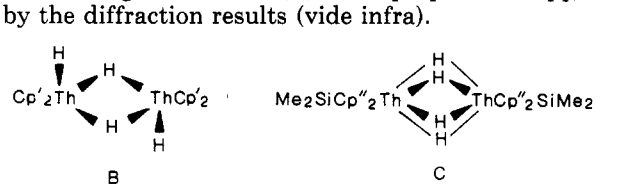

Molecular Structure of $(CH_3)_2Si[\eta^5-(CH_3)_4C_5]_2Th[CH_2Si(CH_3)_3]_2$ (2a). The X-ray structural analysis reveals that single crystals of **2a** are composed of mononuclear, "bent sandwich" $Me_2SiCp''_2Th[CH_2Si(CH_3)_3]_2$ molecules as shown in Figure 1. The molecule possesses

crystallographic C_s—m symmetry with Th, Si_c, C_1, C_2, C_{1a}, Si_a, C_{2a}, C_{1b}, Si_b, and C_{2b} lying in the mirror plane. Final atomic coordinates and anisotropic thermal parameters for non-hydrogen atoms are given in Tables II and III,[16] respectively. Bond lengths and angles are compiled in Table IV employing the labeling scheme in Figure 1. Perhaps the most interesting structural feature of **2a** is the pronounced distortion of the thorium coordination geometry from that typically found in Cp'_2ThX_2 complexes. Thus, the ring center-of-gravity–Th–ring center-of-gravity (Cg–Th–Cg) angle has contracted from typical values in the 135–138° [2,24] range (134.9° in $Cp'_2Th[CH_2Si(CH_3)_3]_2$ (**4**)[33]) to 118.4° in **2a**. The corresponding C_g–Nd–C_g values in $(Me_2SiCp''_2NdCl)_2Cl^-Li(THF)_2^+$ and $Me_2SiCp''_2NdCH[Si(CH_3)_3]_2$ are 121.3° and 121.6°, respectively.[6] The dihedral angle between the C_5 ring mean planes in **2a**, 75°, can be compared to values near 45° for Cp'_2ThX_2 complexes[2,24] (45.8° in **4**[33]). Another consequence of the $Me_2SiCp''_2$ ligation is a marked dispersion in Th–C(ring) distances: average Th–C = 2.791 (15, 84, 126, 4) Å[34] versus 2.81 (1, 1, 4, 10)[34] in **4**.[33] The longest distances are to the ring carbon atoms furthest from Si_c. That Si_c is displaced from each C_5 ring mean plane in the direction of Th by 0.41 Å and that $\angle Cp_1$–Si_c–Cp'_1 = 100.6 (9)° suggests a considerable strain at Si_c imposed by η^5 thorium coordination. The analogous parameters in $(Me_2SiCp''_2NdCl)_2Cl^-Li(THF)_2^+$ are 101.0 (3)°, 0.549 (3) Å, and 0.535 (2) Å.[6] Likewise, the C(ring)–Si–C(ring) angle in $Me_2SiCp''_2NdCH[Si(CH_3)_3]_2$ is 101.2 (8)°.[6] It can also be seen in Table IV that there is a considerable dispersion in the ring C–C distances, ranging from 1.56 (3) Å for Cp_3–Cp_4 to 1.36 (2) Å for Cp_2–Cp_3 and 1.21 (3) Å for Cp_4–Cp_5. Such effects are not typical of Cp'_2ThX_2 complexes.[2,24] Interestingly, the aforementioned neodymium structures evidence little dispersion in C(ring)–C(ring) bond distances. Another consequence of the Me_2Si linkage is a forced eclipsing of Cp″ methyl groups on the chelating rings. Staggered or partially staggered conformations are usually observed in Cp'_2ThX_2 complexes.[2,24]

In regard to the $Th[CH_2Si(CH_3)_3]_2$ ligation in **2a**, the C_{1a}–Th–C_{1b} angle of 98.9 (8)° compares favorably with that of 96.8 (4)° in **4**.[33] The present Th–C_{1a}–Si_a and Th–C_{1b}–Si_b angles of 123.7 (14)° and 149.5 (12)°, respectively, compare favorably with similar angles of 132.0 (6)° and 148.0 (7)°, respectively, in **4**. Likewise, the distances Th–C_{1a} = 2.54 (2) and Th–C_{1b} = 2.48 (2) Å find parallel trends in **4** (2.51 (1) and 2.46 (1) Å for the same types of bonds).[33] Recent neutron diffraction results on $Cp'_2Th[CH_2C(CH_3)_3]_2$[24] as well as theoretical studies[3a] argue that alkyl group distortions as exemplified by the large $\angle$Th–C_{1b}–Si_b are stabilized by agostic interactions between α-C–H bonds (e.g., D) and thorium frontier orbitals in the "equatorial girdle".

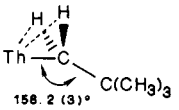

D

That the potential surface for such distortions is rather shallow is argued by the calculations[3a] and by NMR data (vide infra). Ring methyl–alkyl group nonbonded interactions no doubt also influence the disposition of ligands in the equatorial girdle, and for **4**, contacts less than the 4.0 Å sum of methyl van der Waals radii[35] include six C_{1a},C_{1b}–ring methyl distances of 3.43, 3.49, 3.52, 3.66, 3.69, and 3.81 Å and one Si–CH_3–ring methyl distance of 3.76 Å.[33] In contrast, the only short C_α–ring methyl distances in **2a** are C_{1a}–C_{m4} (C_{m4}') = 3.72 Å and C_{1b}–C_{m3}(C_{m3}') = 3.75 Å—significantly longer than above. The shortest Si–CH_3–ring methyl distances are C_{3b}(C_{3b}')–C_{m3}(C_{m3}') = 3.78 Å and C_{3a}(C_{3a}')–C_{m4}(C_{m4}') = 3.89 Å. Another potential descriptor of $Th[CH_2Si(CH_3)_3]_2$ distortions and a possible consequence of the enforced eclipsing of Cp″ methyl groups is the disposition of C_{1a} and C_{1b} with respect to the C_g–Th–C_g' least-squares mean plane. For **2a**, these displacements are +2.12 and −1.67 Å in the direction perpendicular to C_g–Th–C_g plane and are similar to corresponding values of +2.04 and −1.66 Å in **4**.[33] In the sum, the metrical data show that Me_2Si ring chelation has significantly opened the thorium coordination sphere.

Evidence that the potential surface for alkyl group distortion is rather shallow in these complexes comes from ^1H NMR studies that indicate magnetic, equivalence of $Th[CH_2X(CH_3)_3]_2$ groups down to ca. −90 °C.[24a,33,36] Nevertheless, **4** exhibits *two* C_α signals at δ 92.0 and 65.0 in the solid-state ^{13}C CPMAS spectrum versus a single, averaged resonance at δ 76.0 in solution.[24] Complex **2a** exhibits a single solid-state C_α signal at δ 67.2 versus a single resonance at δ 89.52 in solution. With the assumption that the latter is an averaged value, a second C_α

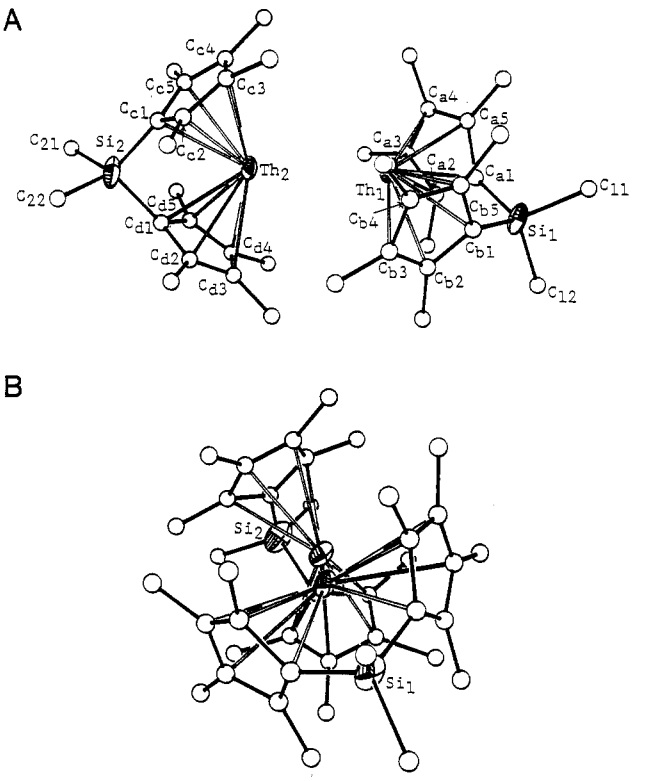

Figure 2. Two views of the molecular structure of $[(CH_3)_2Si[(CH_3)_4C_5]_2ThH_2]_2$ (**3**). Thorium and silicon atoms are represented by thermal vibration ellipsoids drawn to encompass 50% of the electron density; carbon atoms are represented by open spheres. Hydrogen atoms were not located.

(33) Bruno, J. W.; Marks, T. J.; Day, V. W. *J. Organomet. Chem.* **1983**, *250*, 237–246.

(34) The first number in parentheses following an averaged value of a bond length or angle is the root-mean-square estimated standard deviation of an individual atom. The second and third numbers are the average and maximum deviations from the averaged value, respectively. The fourth number represents the number of individual measurements that are included in the average value.

(35) Pauling, L. *The Nature of the Chemical Bond*, 3rd ed.; Cornell University: Ithaca, NY, 1960; p 260.

(36) In the 100-MHz ^{13}C NMR spectrum of $Cp'_2Th[CH_2C(CH_3)_3]_2$, collapse of the C_α resonances is observed by ca. −90 °C, while the other resonances in the complex remain relatively sharp: Smith, G. M. Ph.D. Thesis, Northwestern University, July 1986.

Table V. Atomic Coordinates for Non-Hydrogen Atoms in Crystalline $\{(CH_3)_2Si[\eta^5\text{-}(CH_3)_4C_5]_2ThH_2\}_2$ (3)[a]

atom type[b]	fractional coordinates 10^3x	10^3y	10^3z	isotropic thermal parameters, B,[c] Å^2
Th_1	309.2 (1)	184.0 (1)	71.6 (1)	2.33 (2)
Th_2	299.8 (1)	314.1 (1)	-64.5 (1)	2.58 (3)
Si_1	237.5 (8)	29.0 (4)	148.5 (4)	3.5 (2)
Si_2	249.1 (9)	467.6 (5)	-153.6 (4)	4.0 (3)
C_{11}	306 (3)	-18 (2)	228 (2)	7 (1)
C_{12}	109 (3)	-33 (2)	120 (2)	6 (1)
C_{21}	322 (3)	500 (2)	-236 (2)	7 (1)
C_{22}	146 (3)	542 (2)	-128 (2)	7 (1)
C_{a1}	349 (3)	49 (2)	77 (2)	4 (1)
C_{a2}	325 (2)	61 (2)	3 (1)	4 (1)
C_{a3}	425 (2)	95 (2)	-29 (1)	3 (1)
C_{a4}	517 (3)	101 (2)	23 (2)	4 (1)
C_{a5}	473 (2)	79 (2)	89 (1)	4 (1)
C_{ma2}	214 (3)	40 (2)	-38 (2)	4 (1)
C_{ma3}	439 (3)	117 (2)	-107 (2)	6 (1)
C_{ma4}	639 (3)	134 (2)	17 (2)	5 (1)
C_{ma5}	553 (3)	73 (2)	155 (2)	5 (1)
C_{b1}	173 (2)	113 (2)	170 (1)	3 (1)
C_{b2}	82 (2)	149 (2)	130 (1)	2 (1)
C_{b3}	86 (3)	219 (2)	150 (1)	4 (1)
C_{b4}	185 (2)	227 (2)	197 (1)	4 (1)
C_{b5}	237 (2)	167 (2)	214 (1)	3 (1)
C_{mb2}	-15 (2)	118 (2)	82 (1)	4 (1)
C_{mb3}	2 (3)	272 (2)	122 (2)	5 (1)
C_{mb4}	222 (3)	291 (3)	233 (2)	7 (1)
C_{mb5}	339 (3)	154 (2)	268 (1)	4 (1)
C_{c1}	362 (2)	442 (2)	-83 (1)	4 (1)
C_{c2}	341 (2)	442 (2)	-5 (1)	4 (1)
C_{c3}	439 (2)	403 (2)	23 (1)	4 (1)
C_{c4}	517 (2)	385 (2)	-29 (1)	4 (1)
C_{c5}	474 (3)	410 (2)	-91 (2)	4 (1)
C_{mc2}	247 (3)	474 (2)	37 (2)	5 (1)
C_{mc3}	455 (3)	388 (2)	105 (2)	5 (1)
C_{mc4}	638 (3)	343 (2)	-19 (2)	6 (1)
C_{mc5}	539 (3)	397 (2)	-163 (2)	6 (1)
C_{d1}	164 (2)	385 (2)	-162 (1)	3 (1)
C_{d2}	72 (2)	359 (2)	-110 (1)	3 (1)
C_{d3}	61 (2)	290 (2)	-117 (1)	3 (1)
C_{d4}	136 (2)	272 (2)	-172 (1)	4 (1)
C_{d5}	203 (2)	327 (2)	-202 (1)	3 (1)
C_{md2}	-5 (3)	401 (2)	-62 (2)	5 (1)
C_{md3}	-26 (3)	244 (2)	-85 (2)	5 (1)
C_{md4}	144 (3)	197 (2)	-207 (2)	7 (1)
C_{md5}	297 (3)	327 (2)	-262 (2)	5 (1)

[a] Numbers in parentheses are the estimated standard deviation in the last significant digit. [b] Atoms are labeled in agreement with Figure 2. [c] For the Th and Si atoms this is one-third of the trace of the orthogonalized $\mathbf{B}_{ij}$ tensor; for carbon atoms it is the isotropic thermal parameter that actually refined.

signal at ca. δ 112 is predicted for **2a** in the solid. This field position is exactly coincident with that of the Cp″ ring carbon atoms, so it is likely that **2d** has a solid-state C_α chemical shift dispersion similar to that of **4**.

Molecular Structure of $\{(CH_3)_2Si[(CH_3)_4C_5]_2ThH_2\}_2$ (3). As can be seen in Figure 2, crystals of **3** are composed of dimeric $(Me_2SiCp''_2ThH_2)_2$ units (the hydride hydrogen atoms could not be located with any certainty). Final atomic coordinates and anisotropic thermal parameters for Th and Si are compiled in Tables V and VI,[16] respectively. Bond distances and angles are given in Table VII with labeling according to Figure 2. Within each half of the dimer, metrical parameters are rather similar to the $Me_2SiCp''_2Th$ coordination in **2a**. Thus, C_{ga}–Th_1–C_{gb} = 118.1° and C_{gc}–Th_2–C_{gd} = 117.7°. The dispersion in Th–C(ring) distances is also rather similar (Table VII) with the longest distances (ca. 2.9 Å) to the two ring carbon atoms furthest from the silicon bridges. However, the dispersion in ring C–C distances is less than in **2a** and conforms to no obvious pattern. The Th–Si distances in **3**, 3.487 (9) and 3.517 (9) Å, are similar to that in **2a**, 3.465 (6) Å. The C(ring)–Si–C(ring) angles of 103 (1)° and 99 (1)° in **3** also compare favorably with that in **2a**.

Table VII. Bond Lengths (Å) and Angles (deg) Involving Non-Hydrogen Atoms in Crystalline $\{(CH_3)_2Si[\eta^5\text{-}(CH_3)_4C_5]_2ThH_2\}_2$ (3)[a]

parameter[b]	value	parameter[b]	value
Bond Lengths			
Th_1–Th_2	3.632 (2)	C_{a5}–C_{ma5}	1.52 (4)
Th_1–Si_1	3.487 (9)	C_{b1}–C_{b2}	1.44 (4)
Th_2–Si_2	3.517 (9)	C_{b1}–C_{b5}	1.53 (4)
		C_{b2}–C_{b3}	1.44 (5)
Th_1–C_{a1}	2.72 (4)	C_{b3}–C_{b4}	1.42 (4)
Th_1–C_{a2}	2.78 (3)	C_{b4}–C_{b5}	1.36 (5)
Th_1–C_{a3}	2.89 (3)	C_{b2}–C_{mb2}	1.52 (4)
Th_1–C_{a4}	2.97 (3)	C_{b3}–C_{mb3}	1.50 (5)
Th_2–C_{a5}	2.77 (3)	C_{b4}–C_{mb4}	1.49 (5)
Th_1–C_{b1}	2.77 (2)	C_{b5}–C_{mb5}	1.52 (4)
Th_1–C_{b2}	2.82 (2)	C_{c1}–C_{c2}	1.48 (4)
Th_1–C_{b3}	2.94 (3)	C_{c1}–C_{c5}	1.39 (4)
Th_1–C_{b4}	2.87 (3)	C_{c2}–C_{c3}	1.41 (4)
Th_1–C_{b5}	2.81 (3)	C_{c3}–C_{c4}	1.35 (4)
Th_2–C_{c1}	2.66 (4)	C_{c4}–C_{c5}	1.36 (4)
Th_2–C_{c2}	2.80 (3)	C_{c2}–C_{mc2}	1.46 (4)
Th_2–C_{c3}	2.84 (3)	C_{c3}–C_{mc3}	1.59 (4)
Th_2–C_{c4}	2.84 (3)	C_{c4}–C_{mc4}	1.58 (4)
Th_2–C_{c5}	2.75 (3)	C_{c5}–C_{mc5}	1.55 (4)
Th_2–C_{d1}	2.74 (3)	C_{d1}–C_{d2}	1.49 (4)
Th_2–C_{d2}	2.79 (3)	C_{d1}–C_{d5}	1.43 (4)
Th_2–C_{d3}	2.83 (3)	C_{d2}–C_{d3}	1.38 (5)
Th_2–C_{d4}	2.82 (3)	C_{d3}–C_{d4}	1.37 (4)
Th_2–C_{d5}	2.79 (2)	C_{d4}–C_{d5}	1.44 (4)
C_{a1}–C_{a2}	1.43 (4)	C_{d2}–C_{md2}	1.50 (5)
C_{a1}–C_{a5}	1.50 (4)	C_{d3}–C_{md3}	1.47 (4)
C_{a2}–C_{a3}	1.43 (4)	C_{d4}–C_{md4}	1.63 (6)
C_{a3}–C_{a4}	1.41 (4)	C_{d5}–C_{md5}	1.53 (4)
C_{a4}–C_{a5}	1.39 (4)	Si_1–C_{11}	1.91 (4)
C_{a2}–C_{ma2}	1.49 (4)	Si_1–C_{12}	1.95 (4)
C_{a3}–C_{ma3}	1.53 (4)	Si_2–C_{21}	1.86 (4)
C_{a4}–C_{ma4}	1.50 (4)	Si_2–C_{22}	1.92 (4)
Bond Angles			
C_{a1}–Si_1–C_{b1}	103 (1)	C_{ga}–Th_1–C_{gb}[c]	118.1 (...)
C_{c1}–Si_2–C_{d1}	99 (1)	C_{gc}–Th_2–C_{gd}[c]	117.7 (...)

[a] Numbers in parentheses are the estimated standard deviation in the last significant digit. [b] Atoms are labeled in agreement with Tables V–VI and Figure 2. [c] C_{ga}–C_{gd} designate the centers-of-gravity for the five-membered rings of $(CH_3)_4C_5$ ligands a–d, respectively.

Although the dimer has no crystallographically imposed symmetry elements in space group $P2_1/n$, the overall symmetry approaches C_2 with the idealized 2-fold axis passing through the midpoint of the $Th_1\cdots Th_2$ vector. For example, the least-squares mean planes defind by C_{ga}–Th_1–C_{gb} and C_{gc}–Th_2–C_{gd} intersect with a dihedral angle of 95°. However, as can be seen in Figure 2, atoms Si_1–Th_1–Th_2–Si_2 are not in a direct line, but rather the silicon atoms are displaced 0.13 (Si_1) and 0.18 Å (Si_2) from their respective C_g–Th–C_g planes. This results in $\angle Si_1$–Th_1–Th_2 = 156° and $\angle Si_2$–Th_2–Th_1 = 162°.

Perhaps the most striking feature of **3** is the relatively short Th_1–Th_2 distance of 3.632 (2) Å. This value can be compared to Th–Th distances of 3.60 and 3.44 Å, estimated from twice the thorium metallic radius (12-coordination)[37] and single-bond radius,[38] respectively. It can also be compared to a Th–Th distance of 4.007 (8) Å in $[Cp'_2Th(\mu\text{-}H)H]_2$ (B)[32] and 3.83–4.10 Å in various binary thorium hydrides.[39] Perhaps more relevant to the present thorium

(37) Wells, A. F. *Structural Inorganic Chemistry*, 5th ed.; Oxford University: Oxford, 1984; pp 1286–1288.
(38) Pauling, L.; Kamb, B. *Proc. Nat. Acad. Sci. U.S.A.* **1986**, *83*, 3569–3571.
(39) (a) Rundle, R. E.; Shull, C. G.; Wollan, E. O. *Acta Crystallogr.* **1952**, *5*, 22–26. (b) Zachariasen, W. H. *Acta Crystallogr.* **1953**, *6*, 393–398.

oxidation state and coordination environment is the Th–Th bond distance that can be estimated from the Th–Ru distance in $Cp'_2Th(I)Ru(Cp)(CO)_2$ (Th–Ru = 3.0277 (6) Å).[40] With use of a $CpRu(CO)_2$ radius of 1.42 Å derived from Ru–Ru single-bond distances in similarly ligated binuclear ruthenium complexes[41] and a $Cp'_2Th(I)$ radius of 1.61 Å, a hypothetical Th–Th bond distance of 3.22 Å is estimated. From these metrical considerations, it thus appears unnecessary to invoke extensive direct Th–Th bonding in **3**, but rather the relatively close metal–metal contact is a necessary consequence of the relatively rare (only one other example has been characterized crystallographically[42]) $M(\mu\text{-}H)_4M$ hydride bonding. This in turn must reflect the greater formal coordination numbers available in the $Me_2SiCp''_2Th$ coordination sphere vis-à-vis that in Cp'_2Th analogues. In addition, Ortiz and Hoffmann[43] have shown that the appropriate metal orbitals are available to accommodate a $M(\mu\text{-}H)_4M$ configuration in isoelectronic lanthanide complexes (E). For thorium

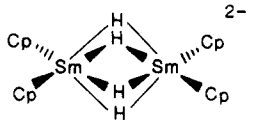

E

complexes, the energy difference between $(H)M(\mu\text{-}H)_2M(H)$ and $M(\mu\text{-}H)_4M$ structures remains unquantified, as does the barrier to their interconversion. That the Th–H ^1H resonances in $[Cp'_2Th(\mu\text{-}H)H]_2$ are magnetically equivalent down to ca. −90 °C suggests that the potential surface must be rather shallow (bridge–terminal hydride interconversions are facile). For **3**, relatively small twists about the Th–Th vector could average what are likely to be minor nonequivalences in bridging hydride environments.

Reactivity. Catalytic Olefin Hydrogenation. The very high catalytic activity of $(Cp'_2MH)_2$ (M = lanthanide, U) and $(Me_2SiCp''_2MH)_2$ (M = lanthanide)[15] complexes for the hydrogenation of simple olefins stands in marked contrast to the behavior of $(Cp'_2ThH_2)_2$.[12] That the reasons might be steric in origin rather than oxidation state or thorium related was explored in studies with **3**.

Olefin hydrogenation experiments utilized apparatus and methodology described elsewhere.[15] Particular attention was paid in kinetic measurements to eliminating mass-transport effects. For the catalytic hydrogenation of 1-hexene by $(Cp'_2ThH_2)_2$ at 25 °C and 1.0 atm of H_2 pressure in heptane or toluene, $N_t = 0.58\ h^{-1}$. In contrast, hydrogenation by **3** under the same conditions proceeds with $N_t = 610\ h^{-1}$—an increase of over 10^3.[44,45] In both cases, GC shows the product to be ≥98% *n*-hexane, and ^1H NMR indicates the recovered hydride catalysts to be ≥98% unchanged. For the aforementioned organolanthanides, in the non-mass-transport limited regime,

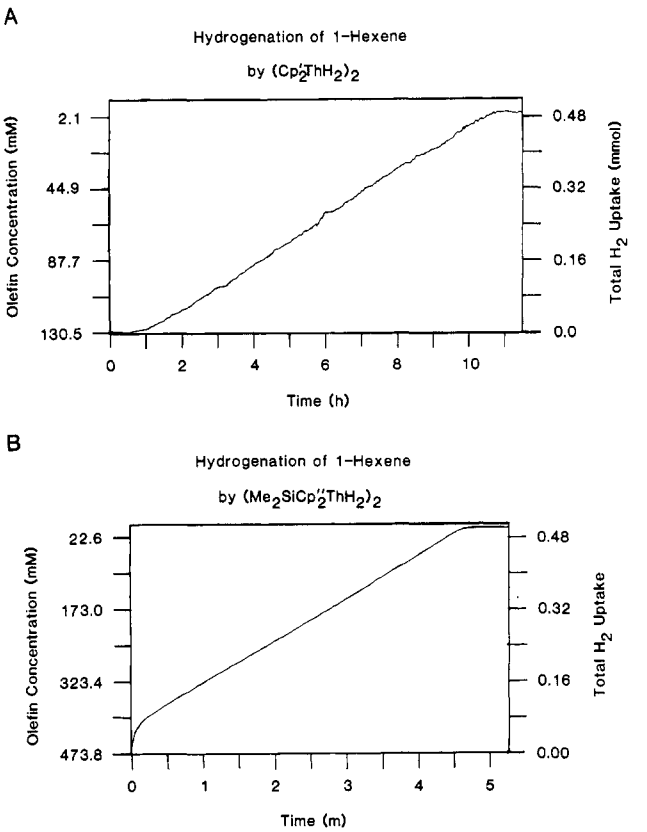

Figure 3. Plots of hydrogen uptake (in mmol) as a function of time during the hydrogenation of 1-hexene at 1.0 atm of H_2 pressure by the following organothorium catalysts in heptane: A, $(Cp'_2ThH_2)_2$, 13.33 mM in Th; B, $(Me_2SiCp''_2ThH_2)_2$ (**3**), 9.39 mM in Th. Both plots illustrate the zero-order dependence of the rate on olefin concentration.

kinetic, NMR, and isotopic labeling data could be accommodated by eq 5–7 where for unhindered olefins such as

$$(LMH)_2 \underset{k_{-1}}{\overset{k_1}{\rightleftharpoons}} 2LMH \quad K_1 \tag{5}$$

$$LMH + \text{olefin} \underset{k_{-2}}{\overset{k_2}{\rightleftharpoons}} LMR \quad K_2 \tag{6}$$

$$LMR + H_2 \xrightarrow[\text{slow}]{k_3} LMH + \text{alkane} \tag{7}$$

1-hexene, k_2 and K_2 are large and $\nu \propto [\text{olefin}]^0[M]^1[H_2]^1$—M–C hydrogenolysis rather than olefin addition is rate-limiting (case A).[15] For bulkier olefins such as cyclohexene (M ≠ Lu), olefin addition is rate-limiting (k_2 is small) and $\nu \propto [\text{olefin}]^1[M]^{1/2}[H_2]^0$ (case B). While the $(Cp'_2ThH_2)_2$, $(Me_2SiCp''_2ThH_2)_2$/1-hexene systems were not investigated as extensively and may be considerably more complex, the data indicate overall kinetic behavior most similar to case A of eq 5–7. Thus, for both thorium complexes, the hydrogenation rate is zero-order in 1-hexene over ≥95% of the reaction course (Figure 3). With the van't Hoff procedure,[46] the reaction is also found to be 1.0(1)-order in thorium for $(Cp'_2ThH_2)_2$ over a 30-fold concentration range and 1.06(2)-order in thorium for $(Me_2SiCp''_2ThH_2)_2$ over a 9-fold (limited by low solubility) concentration range (Figure 4). Measurements of the reaction order in H_2 over the limited pressure range of 0.6–1.5 atm are also in qualitative agreement with case A (nonzero-order in H_2), with the reaction order being 1.0 for $(Cp'_2ThH_2)_2$ and ca. 0.5 for **3**. The latter result suggests

(40) Sternal, R. S.; Brock, C. P.; Marks, T. J. *J. Am. Chem. Soc.* **1985**, *107*, 8270–8272.

(41) (a) Vollhardt, K. P. C.; Weidman, T. W. *J. Am. Chem. Soc.* **1983**, *105*, 1676–1677 (2.821 (1) Å). (b) Behrens, U.; Weiss, E. *J. Organomet. Chem.* **1975**, *96*, 435–450 (2.845 (1) Å).

(42) (a) Teller, R. G.; Bau, R. *Struct. Bonding (Berlin)* **1981**, *44*, 1–82. (b) Wilson, R. B., Jr.; Sattelberger, A. P.; Huffman, J. C. *J. Am. Chem. Soc.* **1982**, *104*, 858–860. (c) Dedieu, A.; Albright, T. A.; Hoffmann, R. *J. Am. Chem. Soc.* **1979**, *101*, 3141–3151. (d) Bau, R.; Carroll, W. E.; Teller, R. G.; Koetzle, T. F. *J. Am. Chem. Soc.* **1977**, *99*, 3872–3874.

(43) Ortiz, J. V.; Hoffmann, R. *Inorg. Chem.* **1985**, *24*, 2095–2104.

(44) These 1-hexene turnover frequencies can be compared with N_t values (25 °C, 1.0 atm of H_2 pressure) of 650 h^{-1} for $Rh(PPh_3)_3Cl$,[45] 4000 h^{-1} for $Ru(COD)(PPh_3)_2PF_6$,[45] 57 000 h^{-1} for $(Cp'_2UH)_2$,[15] 41 000 h^{-1} for $(Me_2SiCp''_2LuH)_2$,[15] and 120 000 h^{-1} for $(Cp'_2LuH)_2$.[15]

(45) Crabtree, R. *Acc. Chem. Res.* **1979**, *12*, 331–338 and references therein.

(46) Laidler, K. H. *Chemical Kinetics*, 2nd ed.; McGraw-Hill: New York, 1963; pp 15–17.

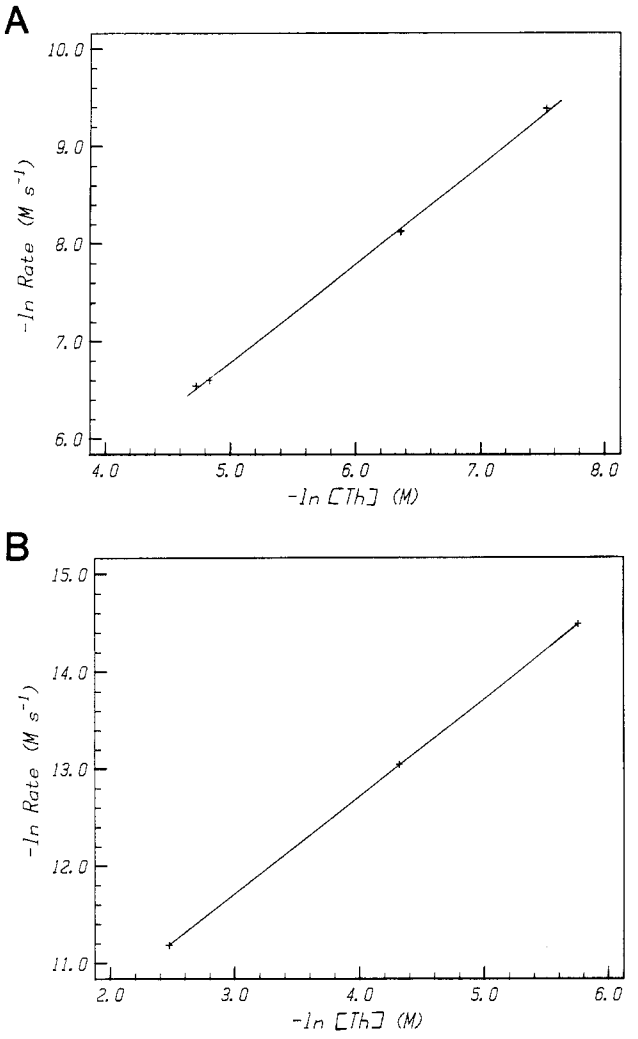

Figure 4. Functional dependence of the observed rate constants on thorium concentration for 1-hexene hydrogenation (1.0 atm of H_2 pressure) by the following organothorium catalysts in heptane: A, $(Me_2SiCp''_2ThH_2)_2$ (**3**); B, $(Cp'_2ThH_2)_2$.

that the mechanism is more complex than described by the limiting case A or B and that more information would ultimately be desirable. ^1H NMR experiments concur that the reaction of these hydrides with α-olefins is both rapid and quantitative. Thermochemical data[47] and thermal stability of **2d** also argue that K_2 is large.

Initial experiments with **3** and *trans*-1-hexene indicate a rate law that is not zero-order in olefin (in contrast to the aforementioned lanthanide complexes[15]). Further mechanistic studies were not carried out; however, comparisons in activity between the two hydrides were made at 1.0 atm of H_2 pressure by using identical hydride (0.017 M) and olefin (0.242 M) concentrations. The result is N_t = 0.086 h^{-1} ($(Cp'_2ThH_2)_2$) and 2.45 h^{-1} (**3**).

These observations demonstrate a significant enhancement in Cp'_2Th-centered olefin hydrogenation rates when permethylcyclopentadienyl ligands are "pulled back". The mechanistic data, do not, however, rigorously establish which of several possible, presumably rate-limiting, four-center heterolytic hydrogenolysis processes[48,49] (eq 8) ac-

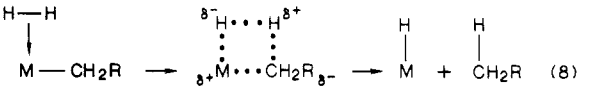

(8)

counts for the acceleration in olefin hydrogenation rate. In related work, we show that the hydrogenolysis of the first Th–C bond in $Me_2SiCp''_2Th(n\text{-}Bu)_2$ occurs only 2–3 times more rapidly than in $Cp'_2Th(n\text{-}Bu)_2$.[48] However, **3** is the only detectable hydrogenolysis product of the former dibutyl compound while the latter forms significant amounts of an intermediate, probably dimeric[50] hydrido alkyl. It is thus conceivable that the principle olefin hydrogenation pathway involves cycling between hydrides and hydrido alkyls.

Conclusions

This work represents a further elaboration of chelating bis(permethylcyclopentadienyl) f-element hydrocarbyl and hydride chemistry. In the present case of tetravalent thorium, as found for trivalent lanthanides, structural features evidence an opening of the metal coordination sphere over that in Cp'_2M analogues. Correspondingly, chemical characteristics evidence a generally enhanced reactivity of metal–carbon and metal–hydrogen σ bonds within the equatorial girdle between the two ring planes. Further studies will probe additional modifications that can be made in the metal coordination sphere and the consequences for chemical reactivity.

Acknowledgment. This research was supported by the National Science Foundation under grant CHE8306255. We thank Dr. P. Toscano for assistance with the CPMAS NMR spectrum.

Registry No. 1, 89597-06-8; **2a**, 89597-09-1; **2b**, 89597-08-0; **2c**, 89618-23-5; **2d**, 89597-07-9; **2e**, 89597-10-4; **3**, 114581-44-1; **3**-*d*, 114581-45-2; $CH_3CH_2C(O)CH_2CH_3$, 96-22-0; CH_3CHO, 75-07-0; Cp''H, 4249-10-9; $Cl_2Si(Cp''H)$, 89597-04-6; $SiCl_4$, 10026-04-7; $Me_2Si(CP''_2H)$, 89597-05-7; $Me_2SiCp''_2Li_2$, 98704-17-7; $Me_2SiCp''_2(MgCl)_2$, 114564-09-9; *i*-PrMgCl, 1068-55-9; $ThCl_4$, 10026-08-1; $(CH_3)_3SiCH_2Li$, 1822-00-0; $(CH_3)_3CCH_2Li$, 7412-67-1; C_6H_5Li, 591-51-5; $C_6H_5CH_2Li$, 766-04-1; $CH_2{=}CH(CH_2)_3CH_3$, 592-41-6; *trans*-$CH_3CH{=}CH(CH_2)_2CH_3$, 4050-45-7; 2,3,5,6-tetrahydro-2,3,5,6-tetramethyl-γ-pyrone, 54458-60-5; 2,3,4,5-tetramethylcyclopent-2-enone, 54458-61-6.

Supplementary Material Available: Tables of anisotropic thermal parameters for non-hydrogen atoms of **2a** (Table III) and **3** (Table VI) (2 pages); listings of observed and calculated structure factors from the final cycle of least-squares refinement (27 pages). Ordering information is given on any current masthead page.

(47) (a) Bruno, J. W.; Marks, T. J.; Morss, L. R. *J. Am. Chem. Soc.* **1983**, *105*, 6824–6832. (b) Sonnenberger, D. C.; Morss, L. R.; Marks, T. J. *Organometallics* **1985**, *4*, 352–355. (c) Nolan, S. P.; Conticello, V. P.; Marks, T. J., unpublished results.

(48) Lin, Z.; Marks, T. J. *J. Am. Chem. Soc.* **1987**, *109*, 7979–7985.

(49) (a) Rabaâ, H.; Saillard, J.-Y.; Hoffmann, R. *J. Am. Chem. Soc.* **1986**, *108*, 4327–4333. (b) Saillard, J.-Y., private communication.

(50) On the basis of the kinetic data, it is also impossible in both the thorium and lanthanide[15] systems to rigorously rule out the importance of completely nondissociating binuclear species as the 1-hexene hydrogenation catalysts. However, the rapidity and exothermicity of the observed hydride + α-olefin addition reactions as well as the higher coordinative saturation expected in hydride-bridged species would seem to mitigate against the importance of such structures.